AFFDL-TR-69-123
VOLUME I

A STABILITY AND CONTROL PREDICTION METHOD FOR HELICOPTERS AND STOPPABLE ROTOR AIRCRAFT

VOLUME I
ENGINEER'S MANUAL

CHARLES L. LIVINGSTON

Bell Helicopter Company
A Textron Company

TECHNICAL REPORT AFFDL-TR-69-123, VOLUME I

FEBRUARY 1970

AIR FORCE FLIGHT DYNAMICS LABORATORY
AIR FORCE SYSTEMS COMMAND
WRIGHT-PATTERSON AIR FORCE BASE, OHIO

DISCLAIMER NOTICE

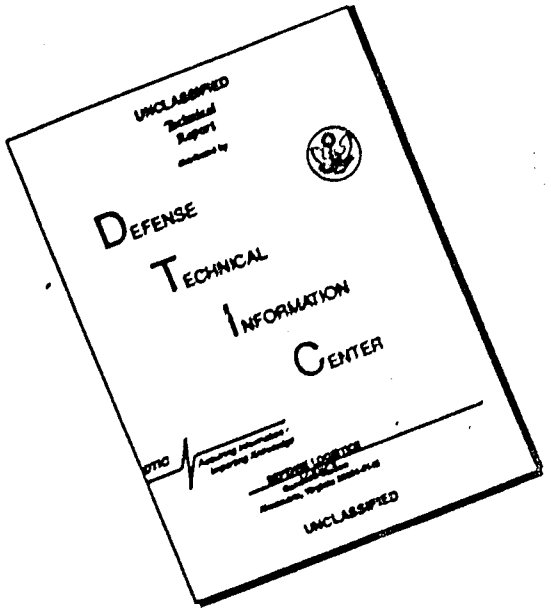

THIS DOCUMENT IS BEST QUALITY AVAILABLE. THE COPY FURNISHED TO DTIC CONTAINED A SIGNIFICANT NUMBER OF PAGES WHICH DO NOT REPRODUCE LEGIBLY.

NOTICE

When Government drawings, specifications, or other data are used for any purpose other than in connection with a definitely related Government procurement operation, the United States Government thereby incurs no responsibility nor any obligation whatsoever; and the fact that the government may have formulated, furnished, or in any way supplied the said drawings, specifications, or other data, is not to be regarded by implication or otherwise as in any manner licensing the holder or any other person or corporation, or conveying any rights or permission to manufacture, use, or sell any patented invention that may in any way be related thereto.

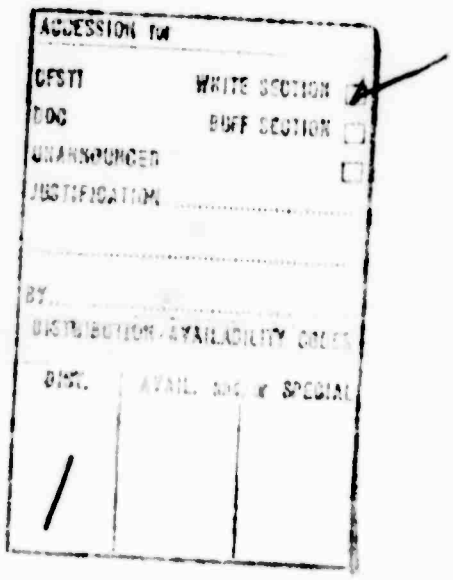

Copies of this report should not be returned unless return is required by security considerations, contractual obligations, or notice on a specific document.

500 - May 1970 - CO455 - 118-2594

A STABILITY AND CONTROL PREDICTION METHOD FOR HELICOPTERS AND STOPPABLE ROTOR AIRCRAFT

VOLUME I
ENGINEER'S MANUAL

CHARLES L. LIVINGSTON

FOREWORD

This report represents the results of the efforts expended in performance of Contract F33615-69-C-1121, "Development of Stability and Control Prediction Methods for Stoppable Rotor Aircraft." The work was performed by Bell Helicopter Company under Project No. 8219. It was sponsored by the Air Force Flight Dynamics Laboratory, Air Force Systems Command, from December 1968 through February 1970. Mr. Charles L. Livingston was the Bell Helicopter Company Project Engineer. Mr. Robert Nicholson was the Air Force Project Engineer.

This final report is presented in four volumes. The first describes the mathematical model and the methods used to calculate stability characteristics. They are of sufficient complexity that a digital computer is necessary for the solution of the equations. The second volume presents the results of sample computations and discusses input and output formats and potential problems. In the third volume, the computer program cross-reference indices are given with explanation of FORTRAN variable and subroutine names. Volume IV is a complete FORTRAN listing of the computer program.

The author gratefully acknowledges the assistance of Messrs. B. L. Blankenship and Tyce McLarty of the Bell Helicopter Company Aeromechanics Group in the development of the mathematical model and of Mr. Bill Bird of the Engineering Computing Group in the programming.

Since the operation of this program requires large computer facilities and the investment of substantial amounts of computer time and manpower, which are not always available for this purpose, Volumes II, III, and IV of this report are not being as widely distributed as the present volume. Organizations desiring copies of those volumes should so inform AFFDL (FDCC), Wright-Patterson AFB, Ohio 45433.

This technical report has been reviewed and is approved.

C.B. Westbrook
Chief, Control Criteria Branch
Flight Control Division
Air Force Flight Dynamics Laboratory

ABSTRACT

This report describes a mathematical model of rotorcraft that may be used to determine characteristics of performance, stability, response, and rotor blade loads. The complexity of the equations used requires the use of a digital computer for efficient solution. This four-volume report describes the computer program in detail and illustrates the method of computing rotorcraft characteristics by specific example.

This volume presents an overview of the computer program capabilities and describes the formulation of the mathematical model. The second and third volumes present sample cases, detailed input and output formats, and cross-reference indices of FORTRAN variable and subroutine names and usage. A complete FORTRAN listing comprises all of the fourth volume.

The computer program was modified from an earlier version so that the stop-fold-rotor concepts could be represented. The two concepts considered are the tilt-forward-trail-aft (TFTA) and the horizontal-stop-fold (HSF) configurations. The TFTA aircraft simulation uses wing-tip mounted rotors for helicopter flight which rotate through 90 degrees to act as propellers in airplane flight. If auxiliary propulsion is available, these rotors may be feathered, stopped, and folded back for high-speed flight. The HSF helicopter simulation uses a conventional main and tail rotor arrangement. The addition of a high-capacity rotor brake enables the rotors to be stopped in flight at a specified location and then folded back through a predetermined schedule. For both of these aircraft, stability and control, performance, and response characteristics may be computed at any time during the conversion maneuvers.

No small angle assumptions are made in the analysis. Aerodynamic interference effects between rotors, wings, elevators, and fins have been represented. First-order elastic effects of the fuselage and wing have been included also. Partial and total stability derivatives may be computed in accelerated or steady flight conditions. Root locations of the rigid-body aircraft motion are computed as well as the transfer functions of the pilot controls. The effects of automatic controls, gusts, and weapon recoil may be easily computed in the form of time histories of motion.

TABLE OF CONTENTS

LIST OF ILLUSTRATIONS

LIST OF TABLES

NOMENCLATURE

A	Airload
A_1	Lateral Cyclic Pitch of Rotor Swashplate
AR	Aspect Ratio
a	Slope of Airfoil Lift Curve
B_1	Longitudinal Cyclic Pitch of Rotor Swashplate
BL	Buttline Reference
b	Number of Rotor Blades, Span, or Width
C	Coefficient
c	Airfoil Chord Length
D	Drag
e	Flapping Hinge Offset in Fraction of Radius
H	Rotor In-plane Force in the $\Psi = 0°$ Direction
K_c	Coning Spring Constant
L	Lift or Roll Moment
l	Length
M	Pitch Moment
m	Blade Mass per Unit Radius
N	Yaw Moment
N_x	Number of Blade Stations
p	Roll Rate
q	Pitch Rate
q'	Dynamic Pressure
R	Blade Radius
r	Yaw Rate
r_b	Radial Distance from Blade Root to Outboard Station
S	Area
SL	Stationline Reference
V	Velocity
WL	Waterline Reference
w	Blade Weight per Segment
X	Longitudinal Axis
XK	Induced Velocity Factor
x	Blade Station Location in Fraction of Radius

NOMENCLATURE

Y	Lateral Axis, Side Force, or Rotor In-plane Force in the $\psi = 90^\circ$ Direction
Z	Vertical Axis
α	Angle of Attack
β	Angle of Sideslip, Mast Longitudinal Tilt Angle, or Blade Flapping Angle
γ	Blade Element Sweep Angle
Δ	Incremental Change
δ_3	Pitch-Flap Coupling
ε	Infinintesimal Change
η	Efficiency
θ	Euler Pitch Angle
θ_1	Rotor Blade Twist Rate
θ_o	Rotor Blade Collective Pitch
λ	Inflow Ratio
μ	Advance Ratio (Forward Speed/Tip Speed)
π	3.14159265...
ρ	Air Density
Σ	Summation
σ	Rotor Solidity Ratio
ϕ	Euler Roll Angle
ψ	Euler Yaw Angle or Rotor Azimuth Position
Ω	Rotor Rotational Speed

Subscripts

b	Rotor Blade
c	Compressible
D	Drag
e	Elevator
eff	Effective
f	Fuselage
h	Hub
i	Induced
L	Lift
m	Mast

Subscripts (Continued)

mom	Momentum Theory
P	Perpendicular to Mast
pc	Precone
R	Parallel to Blade (Radial Direction)
s	Sound
T	Tangential to Blade
w	Wing
x	Direction along X axis
y	Direction along Y axis
z	Direction along Z axis
0	Steady or Trimmed Value
2D	Two Dimensional

SECTION I

INTRODUCTION

Because the equations that describe the physical phenomena are quite complex, and because the mathematical model is designed to represent a wide variety of rotorcraft configurations, stability and control characteristics are calculated by a digital computer. The mathematical model has evolved from a relatively simple rotor-loads analysis over some ten years. As it was refined, the program was carefully checked at each step to ensure that it included all the modifications of the mathematical model. The original rotor-loads analysis emphasized dynamics; later, aeroelastic characteristics were added. The capabilities of the analysis have been demonstrated in published papers, with some sample cases that show the correlation with measured data.[1,2] Adding the aerodynamics of the wing, fuselage, and empennage to the mathematical model of the rotor made the representation of trimmed flight conditions easier and more accurate. Then another section was added to the program to enable it to represent maneuvers. It then became possible to compute the blade loads in maneuvers as well as in trimmed flight.

In 1965, Bell entered into a contract with the U.S. Army Aviation Materiel Laboratories to determine analytically the gust response of rotors.[3] The maneuver section of the analysis was augmented during the performance of this contract to compute response to gusts of any magnitude, from any direction. The gust shapes could be sharp-edged, ramp, or sine-squared. A version of the computer program was delivered to the Army under this contract,[4] and a subsequent version[5] is now operational on the CDC6600 digital computer at the NASA Langley Research Center.

The analysis was further expanded during studies of composite research aircraft to include tilting proprotors and a more sophisticated control system.[6] Concurrently, a subroutine that enabled the computation of partial stability derivatives in trimmed flight was added. Subsequent modifications of the trim analysis included the equations which represent accelerated flight conditions: banked turns, pull-ups, or push-overs; during level, climbing, descending, accelerating, or decelerating flight. The program can now represent a variety of aircraft configurations, including:

- Helicopters

  Single Main and Tail Rotors
  Tandem Rotors
  Laterally-Displaced Rotors
  Compound (jet or propeller propulsion)

- Fixed-Wing Aircraft

    Jet-Propelled
    Propeller-Driven, Single or Twin Engines

- Composite Aircraft

    Tilt-Rotor
    Tilt-Stop-Fold-Rotor
    Edgewise-Stopped-Rotor

The maneuver analysis can also be used to evaluate the effects of a wide variety of inputs and systems on aircraft response. Examples of the kinds of inputs it can handle are gusts, weapon recoil, drop of external stores, control motions, stability augmentation signals, and the commands of rotor-pitch governors.

Sample cases of stop-fold maneuvers have been computed and the resulting time histories are discussed in Volume II, Section IID. These cases are illustrative only and do not represent any particular aircraft configuration.

SECTION II

COMPUTER PROGRAM ORGANIZATION

The computer program is divided into several major sections. The relationships between the major sections are illustrated by the flow chart in Figure 1. The sections of the program which are used in any particular problem are controlled by the input data cards for that section. Therefore, the number of cards of input data required can vary considerably, depending upon how the program is to be used. After the data cards are read, problem constants are computed and parameters are initialized. The functions of the subsequent computational blocks of Figure 1 are discussed below.

A. DETERMINATION OF EQUILIBRIUM FLIGHT CONDITION

The six conventional equations describing aircraft force and moment equilibrium must be satisfied for the trim flight condition. Additionally, the equations describing the longitudinal and lateral moments acting on both rotors must be satisfied. Since the rotor speed is assumed constant, there are ten equations to be satisfied.

The ten unknowns to be determined are: the longitudinal and lateral flapping angles of each rotor, the pilot control positions, and the angular orientation of the aircraft in space. The pilot controls are the collective pitch lever, the longitudinal and lateral cyclic stick, and the pedals. The Euler angle of pitch is always determined by the trim technique and either the roll or yaw angle is computed as determined by the input data. The mathematical techniques used in the trim subroutine are discussed in detail in Section IV. Essentially, the trim problem is one of determining the solution of ten nonlinear equations in ten unknowns.

The equilibrium flight condition may be any one of three conditions described below. For all conditions, the rate of climb or descent must be specified.

1. <u>One-g, Wings-Level Flight</u>

The first, and most common, condition is that of unaccelerated wings-level flight. Trim parameters are computed at a specified roll or yaw angle. At speeds below about 50 knots for helicopters, the yaw angle must be specified (usually zero) so equilibrium is determined by means of roll angle orientation

of the gravity vector. Generally, only a few degrees of roll are required. If the roll angle is set to zero at low speeds, the aerodynamic forces in the yaw moment equation are so small that very large yaw angles may be required to trim. It is possible that no trim solution can be found with zero roll angle input at low speeds. At speeds higher than about 50 knots, either roll or yaw may be specified.

The determination of trim conditions at speeds over 150 knots can be difficult because of the increasingly nonlinear nature of the trim equations caused by rotor stall, compressibility, and reverse flow. The only effective method for overcoming the high speed trim problem to date has been the use of the parameter sweep feature of the program to obtain trim conditions at successively higher speeds. The starting trim parameters at each speed are the final trim values at the preceding lower speed. By reducing the change in speed from 20 knots to 10, 5, or even fewer knots, either a higher speed trim point is obtained, or the reasons trim cannot be obtained will usually be apparent after examination of the preceding trim parameters and their variation with speed.

Probably the most common source of trouble is that the power increases beyond the capability of the anti-torque system of conventional helicopters to counteract. In this case, the pedal control exceeds the travel limits and directional stability is reduced because of tail rotor stall. The user must then do what the pilot does and begin (simulate) a descent on the computer. Simple energy theory provides a fairly accurate estimate of the rate of descent required.

$$R/D = \frac{550}{GW} (HP_{required} - HP_{available}) \text{ ft/sec}$$

2. Push-overs and Pull-ups

The trim parameters may be determined during symmetrical (wings-level) push-overs and pull-ups. Since this maneuver is not one that can be maintained indefinitely, the computed data are just a "snapshot" of the flight conditions existing at a specified instant. Rate of descent in the actual maneuver is never constant, for example, but trim conditions are computed at the rate of descent specified.

The accurate simulation of this maneuver in the trim subroutine is complicated by the capability of the pilot of the helicopter to induce normal accelerations by two controls: the collective pitch lever and the longitudinal cyclic stick. The normal trim technique used in the computer is to adjust these controls simultaneously to attain the desired flight condition. This may not be the way the pilot actually controls the aircraft,

depending upon speed and the amount and direction of normal acceleration desired. Push-over maneuvers induce less than one-g loading and are usually performed by the pilot with the collective pitch lever fixed. Pull-up maneuvers are usually done with the collective pitch lever fixed if the higher g loading will not be maintained very long, that is, for small flight path corrections, or if altitude loss is not significant. If these conditions are not true, then the pilot tends to use collective and cyclic control together. Both of these control techniques may be simulated in the trim subsection. Collective pitch is used alone at very low speeds and in hover to change g loading. This is most easily simulated by varying the gross weight for which trim parameters are being computed. Division by the actual gross weight then gives the desired g-loading.

To simulate simultaneous control usage, the roll angle is set to zero and the g-load required is specified in the input data. The normal trim techniques are used. Trim conditions at less than one-g have always been determined easily by this technique. At higher loadings than about 1.5 g, the above trim technique will fail to converge to a solution. The reasons for this failure to converge have not been determined to date but initial work indicates that this occurs when the main rotor power exceeds the available power. In other words, one can not simulate on the computer a flight condition which is not attainable in flight and expect a solution to be found. There are two ways to obtain the solution at higher g levels; however, both involve a loss of energy. If airspeed must be maintained (kinetic energy), then a rate of descent must be used (loss of potential energy) to reduce the main rotor power requirement and enable higher normal accelerations to be reached. The other method involves loss of airspeed and no change of altitude.

Since the trim equations assume constant airspeed, it is necessary to simulate a longitudinal acceleration, that is, a force, acting through the center of gravity which is equivalent to a power through the familiar energy equation.

$$\text{Force} = \frac{550}{\text{Velocity}} \left(HP_{\text{required}} - HP_{\text{available}}\right)$$

This is done by altering the input data in the following manner:

- Main rotor collective pitch is input directly and the rotor collective pitch is locked. The value used may be the one-g value, or the highest-attainable-g value.

- A single auxiliary jet is located at the center of gravity and oriented along the approximate flight path at the highest-attainable-g condition. Little error results if it is simply oriented along the X-axis.

- The range of jet thrust is specified so that all horizontal forces likely to be needed are available.

- The pilot's collective pitch lever is linked to the auxiliary jet control.

Once this is done the usual set of trim equations is solved, and the required value of jet thrust is determined. This force, when divided by the weight, is representative of the linear deceleration that would be acting on the aircraft in such a high-g flight condition.

3. Banked Turns

Trim parameters may be computed for turning flight. The normal acceleration, bank angle, or turn radius may be specified in the input data. Assuming that the velocity is known, g is the acceleration of gravity, and either n, ϕ, or R are specified; the unspecified quantities are determined by matrix transformation of the Euler angles and velocities. For level turns the transformation matrix may be reduced to the following equations, assuming that yaw angle is zero.

$$n = \sec\phi$$

$$\frac{V^2}{R} = g\sqrt{n^2 - 1}$$

The angular rates of the aircraft about the X, Y, and Z axes are:

$$p = -\frac{g}{V}\sin\theta\sqrt{n^2 - 1}$$

$$q = \frac{g}{nV}\cos\theta\ (n^2 - 1)$$

$$r = \frac{g}{nV}\cos\theta\sqrt{n^2 - 1}$$

These angular rates and normal accelerations are used in the aircraft equations of motion, which are discussed in Section IIIG, to determine the inertial forces required to accurately simulate the flight conditions.

Coordinated banked turns always induce more than one-g loadings, of course. The same difficulties in obtaining the trim solution to high-g turns are encountered as previously discussed for symmetrical pull-ups. The same means of obtaining solutions may be used as described previously.

B. STABILITY ANALYSIS

After determination of the trim parameters, the stability derivatives may be evaluated about the trim point if desired. These derivatives are the total aircraft derivatives with respect to linear and angular velocities and are evaluated in the body axis system. The technique used is to change the trim flight values of linear and angular rates one at a time, by a small amount which is specified by the input data. After a trim value is incremented, the rotor is allowed to re-establish flapping equilibrium with the attendant changes in forces and moments. The forces and moments in other aerodynamic surfaces also change. The trim flight values of forces and moments are then subtracted from the incremented values, and the differences are then divided by the amount of the increment used. The result is the total derivative of force or moment with linear or angular velocity.

This technique of evaluating stability derivatives is accurate as long as the increment size is properly chosen. If too small an increment is used, then errors are caused by small differences of large numbers. If too large an increment is used, then errors are caused by the non-linear character of many of the parameters. That is, the slope of the line between two points which are too far apart differs significantly from the tangent to the curve at the trim point. The effect of increment size on several primary derivatives of longitudinal motion is illustrated in Figure 2. The values of the derivatives are indicated as are the resulting root locations of the short period and phugoid mode. The STAB increment size is the value used in the input data. The correct linear velocity increment is about 2% of the forward velocity. The magnitude of the angular rate increment is always one-hundredth the linear rate increment, and its dimensions are radians per second. For example, if the forward velocity was 200 ft/sec, the linear rate increment should be 4 ft/sec and the angular rate increment would then be .04 rad/sec.

The detailed discussion of the output format of the stability analysis is given in Volume II, Section IIIH. A sample of this output is given in Table I. The first force and moment array is the trim solution. These numbers represent the force (pounds) and moment (pound-feet) contributions of the individual components of the aircraft to the body-axes forces and moments. The second array shows the forces and moments after the w-velocity has been incremented. The third array is the difference between the first two arrays and illustrates the contribution of each component to the w derivative of interest. These data are printed out for the three linear velocities, u, v, and w, as well as the three angular velocities, p, q,

and r. All of the resulting derivatives are summarized for the whole aircraft and for each rotor. An example of these data is given in Table II. The units of the numbers of Table II are pounds, pound-feet, feet per second, and radians per second, as appropriate.

Not all of the computed stability derivatives are currently used in the present analysis. The present analysis uses the standard uncoupled equations of motion which are available in textbooks.[12] The appropriate derivatives of Table II are substituted and the roots of the characteristic equation are determined as are the phase and amplitude relationships defining the mode shapes.[12] The output data computed for the longitudinal and lateral-directional modes of motion are illustrated in Table III.

The derivatives of control motion with respect to forces and moments are obtained from the partial derivative matrix of ten equations in ten unknowns which is used to obtain the trim solution. These derivatives are also used to obtain the numerators of the transfer functions indicated in Table III. These data are often useful in the determination of stability augmentation system parameters.

C. MANEUVERS

The equations of motion listed in Table X and discussed in Section IIIG may be solved in the maneuver section of the program while control motions, automatic systems, or external disturbances may be introduced and their effects computed. This section of the computer program uses the four-cycle Runge-Kutta technique[14] for determining the values of parameters at the next point in time. This section of the program provides full-coupled, nonlinear response data in contrast to the uncoupled, linear data computed in the stability section. The Runge-Kutta technique is described briefly as follows:

1. Accelerations at $t = t_1$ are computed based upon the positions and velocities at t_1.

2. Using the values from step 1, the positions and velocities are computed at $t = t_1 + 1/2\ \Delta t$.

3. Using the positions and velocities of step 2, the accelerations at $t = t_1 + 1/2\ \Delta t$ are computed.

4. Using the positions and velocities of step 1, and the accelerations of step 3, the new positions and velocities at $t = t_1 + 1/2\ \Delta t$ are computed.

5. Using the positions and velocities of step 4, another acceleration at $t = t_1 + 1/2\ \Delta t$ is computed.

6. Using the positions, velocities, and accelerations of steps 4 and 5, the positions and velocities at $t = t_1 + \Delta t$ are computed.

7. Using the positions and velocities of step 6, the accelerations at $t = t_1 + \Delta t$ are computed.

8. The final positions and velocities at $t = t_1 + \Delta t$ are given by the following equations, where P represents position, V represents velocity, A represents acceleration, and the subscript denotes which of the above steps is used to obtain the value.

$$P_{t+\Delta t} = P_1 + \frac{\Delta t}{6}\left[V_1 + V_6 + 2\ (V_2 + V_4)\right]$$

$$V_{t+\Delta t} = V_1 + \frac{\Delta t}{6}\left[A_1 + A_7 + 2\ (A_3 + A_5)\right]$$

1. <u>Time Step Size</u>

The mathematical model of the rotor changes significantly in the maneuver section. The trim and stability sections use twelve azimuth locations to compute airloads. The maneuver section uses as many azimuth stations as there are rotor blades. This fact largely determines the time step that the user must specify in the input data. This time step may be changed during a maneuver in order to reduce computing time. The time step is determined by the following consideration which relates to the accurate solution of the rotor blade equation of motion.

> The time step must be chosen so that neither rotors rotate through more than about 45 degrees of azimuth during the time step.

Since conventional helicopters have tail rotors which turn at about five times the speed of the main rotor, the time step is usually based upon tail rotor speed. For example, the UH-1D uses a main rotor speed of 324 RPM at which the

tail rotor speed is 1643 RPM. Since 45° is one-eighth of a revolution then the largest allowable time step is approximately 60/1643(8) = .00455 seconds; which could probably be rounded off to .005 seconds without encountering difficulty. If the maneuver being performed involved slowing the rotor, then the time step could be increased proportionately as the rotor speed decreased.

2. Output

The output format is detailed in Volume II, Section III. Here will be described briefly what type of data are available to the user from this section. There are two basic types of output data: the maneuver data page which is printed at every nth time point, where n is specified in the input data, and the plots of variables versus time for every mth time point, where m is specified in the input data.

There are up to 266 variables which may be plotted versus time. These variables relate to nearly all combinations of the following:

{linear / angular} {position / velocity / acceleration} of {rotor tip path planes / rotor blades (individual) / all controls / fuselage}

forces / moments / angles of attack / aerodynamic coefficients of {fuselage / wing / fin / elevator / jets / weapon recoil}

Appropriate scaling factors for the variables chosen are determined by the user and up to three variables may be plotted in the same graph. The plotting routine used is a digital one which uses ten inches of paper width and places the time ordinate down the paper. As many pages of paper as may be required by the length of the maneuver are then used at the rate of 66 time points per page. If no plots are desired, then no plot data cards are used.

The other form of the maneuver data is the page of data which may be printed at every time point or at every mth time point. A sample of these data are given in Table IV. These data have been selected as being most pertinent to most maneuvers. The force and moment summary at the bottom of the page is quite useful in determining what components of the aircraft are

generating the forces and moments acting on the aircraft. It should be remembered by the user that the rotor forces are strongly affected by azimuth position and will vary considerably from time point to time point during the maneuver.

3. Capabilities

There are three primary types of inputs which may be simulated to generate maneuvers. These are: control inputs by the pilot, control inputs by simulated automatic systems, and external disturbances. The detailed specification of these inputs are given in Volume II, Section IIA and IIB. Basically, the time histories of control motion or external disturbances are predetermined. The operating constants, such as dead-band, maximum and minimum rates, thresholds, etc. of automatic systems are also predetermined but the actual control output of these systems depend upon the values of position, velocity, and acceleration during the maneuver. Once these input data are defined, the resulting aircraft motion is computed by the maneuver section of the computer program. Any combination of the above inputs may be operating simultaneously during the maneuver. If certain modes of motion are not of interest in a given problem, rotational degrees of freedom may be effectively locked out by using extremely large inertias about the appropriate axes.

There are nine inputs that relate to pilot control actions. These controls are:

1. The four primary controls

   (a) Collective pitch lever
   (b) Longitudinal cyclic stick
   (c) Lateral cyclic stick
   (d) Pedals

2. Power controls

   (a) Rotor torque
   (b) Auxiliary thrust

3. Conversion controls

   (a) Change mast tilt angle (and RPM)
   (b) Change tail rotor into pusher propeller
   (d) Engage rotor brake.

There are eight inputs that relate to functions that would normally be performed by automatic systems. These are:

1. Rotor speed

   (a) Collective pitch governor
   (b) Set speed for governor

2. Rotor attitude

   (a) Flat tracker for main rotor
   (b) Flat tracker for tail rotor
   (c) Rotor fold mechanism

3. Autopilot functions

   (a) Yaw stabilization
   (b) Pitch stabilization
   (c) Sinusoidal control motion

There are five inputs that relate to external disturbances.

1. Gusts

   (a) Vertical ramp-shaped or step-shaped gust
   (b) Vertical sine-squared-shaped gust
   (c) Horizontal ramp-shaped or step-shaped gust
   (d) Horizontal sine-squared-shaped gust

2. Weapon recoil

D. ROTOR AIRLOADS

The present computer program was derived from another program (Reference 5) which contains a detailed aeroelastic representation of the rotor blade. This portion of the program had to be deleted because the mathematical model of the stop-fold-rotor is time-variant and not quasi-static like the model of Reference 5. This time-variant analysis is not compatible with the dynamical representation of the rotor used in Reference 5. The airload data may be printed out at up to 14 specified time points during a maneuver. These data are based upon rigid blades which may assume different coning angles from the flapping hinge point. No provision is made for the effect on blade loads of the type of hub, mass distribution of the blades, or aeroelastic feedback. Provisions for possible addition of these effects have been left in the program.

The aerodynamic parameters of usual interest are printed at each of 20 blade stations for twelve equally-spaced azimuth locations in the trim and stability sections ofthe program. The maneuver section of the program computes parameters at b azimuth stations, where b is the number of blades. Samples of these data are given in Table V for a case with no radial flow represented. If radial flow is used, then two lines per blade station are used to print the data (see Figure 35, Volume II). Complete descriptions of these data are given in Volume II, Section IIIJ.

If airloads are desired only for the trim condition, then the maneuver section of the program must be entered and airloads requested at time t = 0 seconds. The maneuver should be set up with no inputs and terminate at Δt seconds. If airloads are required during a maneuver, the times must be specified in advance. This usually requires the user to compute the maneuver first, examine the data for times when minimum and maximum values of pertinent parameters occur, and then select those times for airload analysis and rerun the maneuver.

E. VECTOR ANALYSIS

The primary purpose of having the capability to oscillate any one of the pilot's controls in a sinusoidal manner is to enable the response computed in the maneuver section to be reduced to vector form. The advantage of this capability becomes apparent when trying to isolate cause and effect relationships of new configurations or in correlating with the results of the linear, uncoupled stability analysis.

The user must specify at what time point the vector analysis is to begin and to end. Generally, two cycles of control excitation is needed before starting the analysis and the analysis is stopped at the end of the third cycle. These start-stop times may vary depending upon the frequency characteristics of the aircraft and of the excitation. The further removed the excitation frequency is from a natural frequency of the aircraft, the sooner the vector analysis may start. Any parameter that may be plotted may also be vectorially analyzed. Basically, all that is done is to fit the computed time history of any parameter, P, with the following equation. The coefficients are chosen to minimize the root-mean-square value of the deviations from the actual curve. The frequence, ω, used is the excitation frequency specified by the user.

$$P = P_o + P_1 \cos(\omega t + \phi_p)$$

The variance is also computed and printed out for each parameter to indicate how good the curve fit is. The variance should be between 0.95 and 1.00, the latter of which represents a perfect fit. A sample analysis is given in Table VI.

Once the maneuver parameters have been determined in vector form, each may be compared to the others in terms of phase angles and magnitudes. This enables direct comparison with the same data computed in the stability section. It also indicates the degree of nonlinearity and coupling that exists for the specified flight condition of the aircraft. If good agreement exists between the phase angles and magnitudes computed by the stability and the maneuver section, then the faster, linear, uncoupled analysis of the stability section may be assumed to be representative of the characteristics of the aircraft.

Another useful relationship may be determined with the parameters in vector form. Any parameter may be expressed as a linear combination of two other parameters provided that neither of the three parameters differ by 0 or 180° in phase angle. This feature is often useful in isolating cause and effect relationships of different phenomena exhibited by new configurations. An example of this analysis is given in Table VI.

SECTION III

DESCRIPTION OF THE MATHEMATICAL MODEL

This section describes the important equations that are used in the mathematical model. It is not intended to be an exhaustive treatment; the FORTRAN listing in Volume IV is the controlling document.

A. FUSELAGE AERODYNAMICS

All aerodynamic data of the fuselage are represented in the stability-axis system. If wind-tunnel data on the rotorcraft to be simulated are available, the force and moment data should be resolved to stability axis. The aerodynamic center of the fuselage must be specified. A sample of such data from a wind-tunnel test is plotted in Figure 3. The lines indicate the fairing for determining the coefficients used in the input-data cards of the computer program. Since no provisions are made for rolling-moment data, the vertical distance between the center of gravity and the aerodynamic center of the fuselage is determined so that the fuselage force produces the required rolling moment. Other fuselage data are input directly from the fitted curves as indicated in Figure 3. If curves are nonlinear, the slope near the point of interest should be used. For example, if pedal control margins are being investigated the curve should be approximated at high sideslip angles instead of zero. If level flight stability data were of interest, then the curves should be fitted near zero sideslip. If wind-tunnel data are not available, the aerodynamic center and other aerodynamic data must be estimated, giving proper consideration to the representation of forces and moments.

The mathematical model of the tilting-proprotor aircraft includes a representation of the movement of the center of gravity as the proprotors convert from helicopter to airplane mode. The change in drag area and the pitching moment induced by pylon drag are also represented. The input value of center-of-gravity location assumes that the pylons are in the helicopter configuration. The value of pylon flat-plate drag area represents the difference in drag with the masts vertical and horizontal.

The equations used in the representation of fuselage characteristics are summarized in Table VII.

To simplify the nomenclature, the variables that are taken from the input data are represented by their FORTRAN names. The user's guide (Volume II) defines these symbols in more detail.

B. AIRFOIL AERODYNAMICS

The standardized input data on three cards are used to compute the coefficients of lift, C_L, and drag, C_D, as a function of angle of attack and Mach number. In the following discussion YXXI refers to the Ith aerodynamic input for the appropriate aerodynamic surface YXX, as defined in Table VIII. Except for sections specifically labeled otherwise, formulas and procedures apply to all aerodynamic surfaces; i.e., rotors, wings, elevators, or fins.

1. Lift Characteristics

If the lift slope for zero Mach number, input YXX17, is zero, the program will compute C_L and C_D from data tables for a 64A210 airfoil. If input YXX17 has a nonzero value, C_L and C_D will be computed from the analytical and empirical equations described in the following discussion. The airfoil section characteristics included in the aerodynamic input listed in Table VIII are for a two-dimensional symmetrical section at zero Mach number. These input values are corrected by the program to obtain the three-dimensional characteristics for an unswept, symmetrical surface. The form of the computed three-dimensional characteristics are illustrated in Figure 4.

a. Angle of Attack Effects

The current equations represent only symmetric airfoil sections. The same equations may be used for positive and negative angles of attack; since for symmetric sections negative angles of attack produce the same magnitude of lift coefficients as positive angles, only of opposite sign. Thus, only angles of attack between 0 and 180 degrees need be considered when evaluating the operations for C_L. This angle of attack range is divided into two major flow regions, normal ($0° \leq \alpha \leq 90°$) and reverse ($90° < \alpha \leq 180°$) flow, which utilize the same equations but require separate input data.

The normal and reverse flow regions are further divided into three operating regions:

(1) The region where lift is linearly proportional to angle of attack, i.e., $0° \leq \alpha < \alpha_{stall}$.

(2) The stalled region where flow separation has occurred over part of the upper surface, i.e., $\alpha_{stall} \leq \alpha \leq \alpha_B$.

(3) The region where the surface can be considered to be a flat plate, i.e., $\alpha_B < \alpha \leq 90°$.

The boundaries of these regions defined as α_{stall} and α_B are determined internally in the program. The first of these, α_{stall}, is defined as the three-dimensional angle of attack at which $C_L = C_{L_{max}}$ for the Mach number under consideration. The other limit, α_B, is defined as the stall angle of attack at M = 0 plus 5 degrees. If α_B is greater than 40 degrees, it is reset to 40 degrees, and $C_{L_{max}}$ at M = 0 is adjusted so that α_{stall} = 35 degrees.

b. Mach Number Effects

To provide the best approximation of experimental data, different sets of equations are used to compute C_L in the subsonic, transonic, and supersonic regions. The boundaries of three Mach regions are defined as:

(1) Subsonic: $0 \leq M \leq YXX1$

(2) Transonic: bounded by YXX1 on the lower end, and the maximum of either YXX2 or the value of Mach number that satisfies the following condition

$(YXX18)\sqrt{M^2 - 1} = 1$ on the upper end.

(3) Supersonic: bounded only on the lower end by the value coincident with the upper boundary of the transonic region.

The value of C_L below the stall angle is computed as a linear function of the two-dimensional lift curve slope, a_{2D}, and the effective angle of attack, α,

$$C_L = a_{2D}\alpha$$

where $\alpha = \alpha_G - \alpha_i$ and α_G is the geometric angle of attack and α_i is the induced angle of attack.

The program computes the lift curve slope by one of the following equations, depending upon the Mach number. The two-dimensional lift curve slope, YXX17, is corrected for compressibility effects at subsonic speeds by the Prandtl-Glauert correction:

$$a_{2D_c} = \frac{YXX17}{\sqrt{1 - M^2}}$$

For the supersonic region, the lift curve slope is computed from the small perturbation theory equation:

$$a_{2D} = \frac{4}{\sqrt{M^2 - 1}}$$

For the transonic region, the value of lift curve slope is determined from a second-order polynomial curve in Mach number that satisfies the following conditions:

(1) The value of the lift curve slope at the boundaries of the region must equal the values computed at these points by the equations for the adjacent region.

(2) The slope of the lift curve slope versus Mach number curve at the common boundary of the transonic and supersonic region must be continuous with Mach number.

These constraints on the lift curve slope provide continuous values of lift curve slope with Mach number, and result in a discontinuity in the slope of the lift curve slope versus Mach number curve only at the input Mach number of YXX1.

The lift coefficient for the angle of attack region where the surface can be considered to be a flat plate, $\alpha_B \leq \alpha \leq 90°$, is computed from the following empirically derived equation:

$$C_L = \left[\left(2K_1 \sin\alpha - K_2\right)K_3 + 0.81\right]\cos\alpha$$

The values of the constants K_1 and K_2 are selected internally, with different values being set for the rotor and for fixed surfaces.

$$K_1 = \begin{cases} 0.938 \text{ for the rotor} \\ \text{YXX3 or YXX7 for fixed surfaces for normal and reverse flow respectively} \end{cases}$$

$$K_2 = \begin{cases} 0.581 \text{ for the rotor} \\ 0.81 \text{ for fixed surfaces} \end{cases}$$

The constant K_3 is selected independently of the type of surface, but is computed from one of the following equations depending upon the Mach number and angle of attack.

$$K_3 = \begin{cases} 1 + 0.25M^4 & \text{if } M \leq 1 \text{ and } \alpha > \alpha_B \text{ or for computing the value of } \alpha_B \\ 0.84 + \dfrac{0.082}{M - 0.8} & \text{if } M > 1 \text{ and } \alpha \geq \alpha_B \end{cases}$$

The lift coefficient in the angle of attack range between α_{stall} and α_B is determined by linear interpolation between the values of C_L at α_{stall} and C_L at α_B.

c. Induced Angle of Attack

In all of the Mach number and angle of attack regions, the induced angle of attack is considered to be proportional to the coefficient of lift. The expression for induced angle of attack was derived from Prandtl's momentum theory as modified to better represent experimental data. This expression is in the form of one of the following equations:

$$\alpha_i = \left(\frac{YXX17}{YXX17 + \frac{2}{3}\pi YXX18}\right)\alpha \qquad \text{if } \alpha \le \alpha_{stall}$$

$$\alpha_i = \frac{C_L}{\frac{2}{3}\pi(YXX18)} \qquad \text{if } \alpha > \alpha_{stall}$$

For elevators and fins an additional correction is made to C_L to account for the effects of tail boom bending. This correction is accomplished by the following equation:

$$C_L = \frac{C_L}{\left[1 + (YXX11)\left(\frac{C_L}{\alpha_{3D}}\right)A_t q_t\right]}$$

where

A_t = area of the surface

q_t = dynamic pressure at the surface.

2. Drag Characteristics

The equation utilized for the computation of the coefficient of drag, C_D, is dependent on the Mach number. The three Mach ranges for C_D are: subsonic, $0 \le M < 1$; transonic, $1 \le M < M_s$; and supersonic, $M > M_s$, where M_s is the lower boundary of the supersonic range.

a. Unstalled Flow

At subsonic Mach numbers, the airfoil is considered to be operating either unstalled, $0 \le \alpha \le \alpha_{sx}$, or as a stalled flat plate, $\alpha_{sx} < \alpha \le 90°$, where α_{sx} is defined as the minimum of either α_{stall} or the value of α that satisfies the condition that the unstalled drag equation be equal to the input YXX16. This second limiting condition is applied so that the subsonic value of C_D does not exceed the transonic value of C_D and result in a discontinuity.

When $0 \leq \alpha \leq \alpha_{sx}$, the drag coefficient is computed from a second order polynominal in α, the coefficients of which are input data. The equation used is:

$$C_D = \frac{YXX12}{\sqrt{1 - M^2}} + YXX13\alpha + YXX14\alpha^2 + CD3$$

The term CD3 is an empirically derived term added to C_D to account for the effects of Mach number on C_D. This term results in the characteristic drag divergence with increasing angle of attack and Mach number. This term is defined as:

$$CD3 = \max\left\{\begin{matrix}0.0 \\ \max\left\{\begin{matrix}M \\ 0.35\end{matrix}\right\}\end{matrix}\right. - YXX1 + 0.0332\alpha$$

b. Stalled Flow

When $\alpha_{sx} < \alpha \leq 90$, it is necessary to use separate equations for the rotor and for fixed airfoils. For fixed airfoils such as the elevators and fins, C_D may be represented by:

$$C_D = (\alpha - 90)^2\left[\frac{CD_{sx} - 2.0}{(\alpha_{sx} - 90)^2}\right] + 2.0$$

This empirical equation yields a parabolic curve, which is concave downward. It has a value of CD_{sx} at α_{sx} and a maximum value of 2.0 at 90 degrees. The value of CD_{sx} is the minimum of either YXX16 or the value of C_D computed from the unstalled equation for α_{sx}. The maximum of C_D at 90 degrees, 2.0, was selected as being representative of a flat plate perpendicular to the flow. Because of the limiting value for C_D at 90 degrees, it is necessary to limit the value of YXX16 to values less than or equal to 2.0 in order to maintain the proper shape of the C_D versus α curve.

For the rotor sections operating in the α range where $\alpha_{sx} < \alpha \leq 90^\circ$, the equation for C_D is:

$$C_D = CD4\sin^2\alpha + \left[\frac{CD_{sx} - CD4\sin^2\alpha_{sx}}{\cos\alpha_{sx}}\right]\cos\alpha$$

where

$$CD4 = 2.1\begin{cases}1 + 0.25M^4 & \text{for } M \leq 1 \\ 0.84 + \dfrac{0.082}{M - 0.8} & \text{for } M > 1\end{cases}$$

For the range of Mach numbers where $M \geq 1$ but less than the lower boundary of the supersonic region, C_D has a constant value, equal to YXX16, regardless of the value of α.

When the value of Mach number is greater than the lower boundary of the supersonic region, the value of C_D, for all values of α, is the minimum of either YXX16 or that determined by the following equation:

$$C_D = \frac{4(\alpha^2 + YXX15)}{\sqrt{M^2 - 1}} + YXX12$$

C. ROTOR REPRESENTATION

The aerodynamic characteristics of two rotors may be represented in the computer program. Depending on the input-data values, the two rotors can be used as

- A vertical-thrusting main rotor and a right-thrusting tail rotor
- Side-by-side, contra-rotating main rotors
- Tandem, contra-rotating main rotors

In the latter two configurations, the input data for the Tail-Rotor Group applies to the left or aft rotor. Much of the input data and all the analysis are the same for both rotors, so the same description applies to both. All the aerodynamic equations are written in the mast-axis system. Infinitely stiff blades are assumed, with a variety of available hub geometries:

- Rigid, with a virtual hinge point
- Spring-restraint (nonisotropic)
- Gimbaled
- Flapping-hinge-offset
- Focused-pylon

The basic method used to compute the rotor forces, moments, and power required uses conventional blade-element theory.[7,8] A maximum of 20 evenly-spaced blade stations may be represented. Twelve azimuth stations are used in the trim and stability sections of the program. The maneuver section uses as many azimuth stations as blades. The number of blades (of rectangular planform), as well as the blade radius and chord, are specified.

1. Special Provisions

Each blade segment is assumed to be untwisted, but each may have a different incidence with respect to the hub. Linear twist is represented by 20 finite values of blade pitch which are input on the fifth, sixth and seventh data cards in the rotor group. The values to be input are given by:

$$\theta = \theta_{root} + \theta(x)$$

where the inputs are made from the tip of the blade (x = 1) to the root (x = 0). Since the pitch of most rotors is less at the tip than at the root, the input values are normally negative. For example, the UH-1B rotor has a 10-degree "washout" of pitch from root to tip. Thus, for a 20-segment rotor,

```
XMR29 = -10.0     (blade tip, x = 1.0)
XMR30 = - 9.5     (x = 0.95)
XMR31 = - 9.0     (x = 0.90)
   :
   :
XMR47 = - 1.0     (x = 0.10)
XMR48 = - 0.5     (x = 0.05)
```

Precone is accurately represented by the program. The input value is the amount of precone built into the hub. The actual coning angle is computed using a quasi-static balance among centrifugal-force moment, airload moment, and coning-spring moment, represented as follows:

$$\sum_{i=1}^{n_x} r_b^i L^i \left(\Delta r_b^i\right) - \Omega^2 \sin\beta_0 \sum_{i=1}^{n_x} \left[\left(r_b^i\right)^2 \cos\beta_0 + e r_b^i\right] m^i \left(\Delta r_b^i\right) - K_c X_0 = 0$$

The Newton-Raphson iteration technique is used to find a new value of X_0 for each pass through the rotor analysis. After convergence, X_0 represents the coning deflection of the blade from that value of coning angle which is specified by the input data thus, $\beta_0 = \beta_{pc_{input}} + X_0$.

Provisions are made for blade-pitch change with coning as well as with flapping relative to the mast. The use of hub-drag coefficient improves the correlation of computed and flight-test data for stick positions and gradients in forward flight. A first-order approximation of a nonuniform induced-velocity distribution is possible by use of a coefficient for tip-vortex effect. This effect does not influence total rotor forces and power, but it does affect the spanwise and azimuthal distribution of airloads. It is represented by:

$$V_h = \sqrt{V_x^2 + V_y^2} \quad \text{(velocity of the hub in the X-Y plane)}$$

Depending on the values of V_h and Ω, a value of XK is determined for later use by whichever equation below is true first.

$XK = 0.5$	if $\Omega < 1$
$XK = 11.25\ V_h/\Omega R$	if $V_h/\Omega R < 0.1067$
$XK = 1.36 - 1.5\ V_h/\Omega R$	if $V_h/\Omega R < 0.5733$
$XK = 0.5$	if $V_h/\Omega R \geq 0.5733$

A correction factor to the momentum theory value of induced velocity is then computed as follows:

$$xy = V_{i_{mom}}\, XK(XMR27)\sqrt{-\frac{V^2}{2} + \sqrt{\frac{V^4}{4} + V_i^2}}$$

Rotor induced velocity, $V_{i_{mom}}$, is determined from the induced velocity subroutine (9) which is based on momentum theory (10) with empirical corrections so that a value of induced velocity is assured for all rotor operating states.

The input variable XMR27 should be zero if tip vortex effect is not desired and should be unity if it is desired. The second term of the equation below which involves xy is imposed upon the induced velocity distribution only in the azimuth intervals between 45 to 105 degrees and 255 to 315 degrees and only outboard of the 70% blade station.

$$V_i = V_{i_{mom}}\left[1 - \frac{4}{3}x(1 + XK\cos\psi)\right] + xy\ \sin[6(\psi - 45°)]$$

where x is the fraction of blade radius, r_b/R.

2. Blade-Element Aerodynamics

The angle of attack, α, and the sweep, γ, at a specified blade station, r, and azimuth station, ψ, is computed using the following equations:

$$\alpha = \theta + \phi$$

where

$$\theta = \theta_0 - \tan^{-1}\left[\cos\psi\tan A_1 + \sin\psi\tan B_1\right] - \left(\beta-\beta_{pc}\right)\tan\delta_3$$

and ϕ is determined by resolving wind vectors as follows:

The three components of velocity at a blade element, illustrated in Figure 5, are computed by:

$$U_P = \lambda\Omega r_b\cos\beta - r_b\dot{\beta} - (V_{x_h}\cos\psi - V_{y_h}\sin\psi)\sin\beta + U_{P_{gust}}$$

$$U_T = \Omega r_b\cos\beta + V_{x_h}\sin\psi + V_{y_h}\cos\psi - U_{T_{gust}}$$

$$U_R = -\lambda\Omega r_b\sin\beta - (V_{x_h}\cos\psi - V_{y_h}\sin\psi)\cos\beta + U_{R_{gust}}$$

where $\lambda = (V_{z_h} - V_i)/\Omega R$

Gust velocities are determined by the following equations:

Letting G_H, G_V, and G_Y b the longitudinal, vertical, and lateral velocities of th gust, respectively, and defining $G_I = G_H\cos\psi - G_Y\sin\psi$, the gust components are given by:

$$U_{P_{gust}} = G_I\sin\beta - G_V\cos\beta$$

$$U_{T_{gust}} = G_H\sin\psi - G_Y\cos\psi$$

$$U_{R_{gust}} = G_I\cos\beta + G_V\sin\beta$$

The variables V_{x_h}, V_{y_h}, and V_{z_h} are the velocities at the rotor hub caused by airframe linear and angular velocities, mast orientation, and aircraft attitude in space. Let the components in body reference of free-stream velocity be V_x, V_y, and V_z; the angular rates of the body be p, q, and r; and the linear distances from the center of gravity to the rotor hub be l_{x_h}, l_{y_h}, and l_{z_h}, all of which are referenced to the X, Y and Z axes, respectively. The linear velocity at the rotor hub caused by angular velocities is given by

$$V_{x_r} = ql_{z_h} - rl_{y_h}$$

$$V_{y_r} = rl_{x_h} - pl_{z_h}$$

$$V_{z_r} = pl_{y_h} - ql_{x_h}$$

To these values are added the free stream velocity components. The total velocity in body reference is then:

$$V_x = V_{x_r} + V_{x_{body}}$$

$$V_y = V_{y_r} + V_{y_{body}}$$

$$V_z = V_{z_r} + V_{z_{body}}$$

where $V_{y_{body}}$ is corrected for the input value of sidewash coefficient for the tail rotor of the conventional helicopter configuration.

The final transformation requires the orientation of the mast relative to the body to be known. Mast yaw angle is currently set to zero. Mast pitch angle is determined by input data as pretilt, for a conventional helicopter, or conversion angle, for the tilt-proprotor aircraft, and is zero when perpendicular to the X - Y plane of the aircraft. Mast roll angle is zero for the tilt-proprotor and tandem configurations and for the main rotor of the conventional helicopter configuration. The roll angle is 90 degrees for the tail rotor of the conventional helicopter. Defining ϕ_m and θ_m as the mast roll and pitch angle, the free stream velocity components at the hub in the shaft reference system are given by the following equations.

$$V_{x_h} = V_x \cos\theta_m - V_z \sin\theta_m$$

$$V_{y_h} = V_x \sin\phi_m \sin\theta_m + V_y \cos\phi_m + V_z \cos\theta_m \sin\phi_m$$

$$V_{z_h} = V_x \cos\phi_m \sin\theta_m - V_y \sin\phi_m + V_z \cos\theta_m \cos\phi_m$$

These velocities are then used in the preceding equations for U_P, U_T, and U_R at the blade element. The inplane and total velocities are then calculated by:

$$U_I = \sqrt{U_T^2 + U_R^2}$$

$$U = \sqrt{U_I^2 + U_P^2}$$

Radial flow is treated by obtaining two lift and two drag coefficients. One pair of coefficients is resolved in the conventional manner for rotor analysis. The other pair is associated with radial flow and act as if the freestream velocity were parallel to the blade. The conventional angle of attack is determined using an inflow angle, ϕ, from the following equation. Defining sweep angle, γ, as:

$$\tan\gamma = \left|\frac{U_T}{U_R}\right|$$

the inflow angle is

$$\tan\phi = \frac{U_P}{U_T}\sin^2\gamma$$

and so,

$$\alpha = \theta - \phi$$

$$M = \frac{U}{V_S}\sin^2\gamma$$

where ϕ is placed in the proper quadrant, depending upon the sign of U_P and U_T. For no radial flow, U_R is zero and γ is 90 degrees so the equation for ϕ is the same as conventional rotor theory. The lift coefficient, C_L, and drag coefficient, C_D, are obtained from either the airfoil data tables or from the equation subroutine described in the preceding section of this report.

The lift and drag coefficients associated with radial flow are obtained from the same data tables or equations. The angle of attack for radial flow is defined as:

$$\tan\alpha_R = \frac{U_P}{U_R}\cos^2\gamma$$

and the Mach number is

$$M = \frac{U}{V_S}\cos^2\gamma$$

After the lift coefficient is obtained it is modified by the input value in XMR26, which should be between 0 and 10 as follows

$$C_{L_R} = C_L \left[\frac{XMR26\ 2\pi\ c}{57.3(c + 4R)} \right]$$

where c is the rotor chord length.

The radial lift and drag coefficients are represented by C_{L_R} and C_{D_R} respectively. All lift and drag vectors are assumed to be aligned perpendicular and parallel to the local relative wind.

The lift and drag coefficient vectors are then resolved parallel and perpendicular to the blade to obtain net coefficient vectors in the lift, drag, and radial directions. The equations used for the nth blade segment are as follows:

$$A_L = U\left[\sin^2\gamma\left(C_L U_T + C_D U_P \sin^2\gamma\right) + \cos^2\gamma\cos\theta\left(C_{L_R} U_R + C_{D_R} U_P \cos^2\gamma\right)\right]$$

$$A_D = U\left(C_D U_T - C_L U_P \sin^2\gamma\right)\sin^2\gamma$$

$$A_R = U\cos^2\gamma\cos\theta\left(C_{D_R} U_R - C_{L_R} U_P \cos^2\gamma\right)$$

Total rotor forces and power are obtained by summing these airloads along each blade as follows:

$$\text{Thrust} = \frac{\rho c b R}{2N_r N_\psi} \sum_{i=1}^{N_\psi} \sum_{n=1}^{N_r} \left(A_L \cos\beta - A_R \sin\beta\right)$$

$$\text{H-Force} = \frac{\rho c b R}{2N_r N_\psi} \sum_{i=1}^{N_\psi} \sum_{n=1}^{N_r} \left[A_D \sin\psi - \left(A_L \sin\beta + A_R \cos\beta\right)\cos\psi\right]$$

$$\text{Y-Force} = \frac{\rho c b R}{2N_r N_\psi} \sum_{i=1}^{N_\psi} \sum_{n=1}^{N_r} \left[-A_D \cos\psi - \left(A_L \sin\beta + A_R \cos\beta\right)\sin\psi\right]$$

$$\text{Torque} = \frac{\rho c b R}{2N_r N_\psi} \sum_{i=1}^{N_\psi} \sum_{n=1}^{N_r} A_D r$$

N_r is the number of blade stations and N_ψ is the number of azimuth stations. N_ψ equals twelve in the trim and stability sections of the program and is equal to the number of blades in the maneuver section.

3. Blade Motion Equation

The basic differential equation of blade motion considers the effects of shaft angular rates, blade weight and inertia, nonisotropic hub spring restraint, offset flapping hinges, and blade airloads. The flapping acceleration vector is computed for each blade from the following equation.

$$\ddot{\beta}_j = (\cos\beta + \eta)\left(p_m\cos\psi - q_m\sin\psi\right)\cos\beta \qquad \text{(gyroscopics)}$$

$$- \frac{1}{I_b}\left[K_{h_{F/A}}\cos^2\psi + K_{h_{LAT}}\sin^2\psi\right] \qquad \text{(spring restraint)}$$

$$- \Omega^2(\cos\beta + \eta)\sin\beta \qquad \text{(centrifugal force)}$$

$$+ \frac{\rho cR}{I_b N_r}\sum_{i=1}^{N_r} A_{L_i} r_{b_i} \qquad \text{(airload moment)}$$

$$- \frac{1}{I_b}\sum_{i=1}^{N_r} w_i r_{b_i}\left[\sin\beta\left(\sin\psi\cos\theta_{m_{ground}}\sin\phi_{m_{ground}} + \cos\psi\sin\theta_{m_{ground}}\right) + \cos\beta\cos\theta_{m_{ground}}\cos\phi_{m_{ground}}\right] \qquad \text{(weight moment)}$$

where $\eta = \frac{e}{I_b}\int_0^R r_b m dr$

The blade accelerations are added vectorially to obtain a resultant acceleration magnitude and orientation of the rotor disk. The projections of this resultant vector on each blade is then used to determine the flapping acceleration of the blade. This acceleration for the ith blade is given by:

$$\ddot{\beta}_i = \sum_{j=1}^{b} \ddot{\beta}_j \cos\,(j - i)\Delta\psi$$

where $\Delta\psi$ is the azimuth angle between blades.

4. Geometry

The location of the rotor hub must be known for purposes of resolving forces about the center of gravity. This requires the mast pivot point and mast length to be specified for configurations which use tilting rotors. For conventional helicopter configurations, the shaft pivot point location should be the rotor hub location and the mast length should be input as zero. The mast tilt angle must be correctly specified so that flapping is accurately represented.

The blade weight distribution needs to be accurately represented so that the correct center of gravity shift is computed during blade folding. Also, the total blade inertia about the flapping axis must be accurately represented if meaningful rotor stability derivatives with respect to angular rates are to be obtained. A prior version of the computer program (1,4) included a dynamic analysis of the rotor blade and included blade deflections and deflection velocities in the aerodynamic representation. This capability of the program had to be deleted in order to accommodate the additions required to represent the stop-fold rotor concepts. The blades are currently represented as rigid airfoils that are free to flap but not deflect.

D. FIXED AERODYNAMIC SURFACES

All of the fixed aerodynamic surfaces represented in the computer program utilize lifting line theory with corrections made for aspect ratio. The center of pressure location of each surface must be specified by the input data. The airfoil aerodynamics subroutine discussed previously is used to determine lift and drag coefficients at the angle of attack and Mach number of the airfoil. The wing and elevator are assumed to be mounted horizontally and the fin is assumed to be mounted vertically.

1. Wing

The wing area, aspect ratio, two-dimensional lift curve slope, maximum lift coefficient, angle of incidence of the zero lift line relative to the fuselage waterline, and center of pressure location of the right panel are the more important input parameters. Wing side force and pitching moment are not represented by the computer program. If a cambered airfoil section is used, the resultant pitching moment should be included in the data of the fuselage.

The wing area used should be the total area of the wing as shown in a top view, including fuselage carry-through. In the event that relatively "stubby" wings are used and no wind

tunnel data are available to provide corrective data, the following correction to the slope of the wing lift curve should provide an accurate representation of first-order wing-body interference effects:(11)

$$a_w = a_{w_{2D}}\left[1 - \left(\frac{b_f}{b_w}\right)^3\right]$$

where b_f is the width of the fuselage and b_w is the span of the wing. The above value of lift curve slope should be used for the two-dimensional lift curve slope which is specified by the input data. If no wing is used, a zero should be input as the value of wing area.

The wing contributions to roll and yaw moment are computed using the values of stability derivatives which are input to the program. If these stability derivatives are not known from flight or wind tunnel test, they may be easily estimated using standard techniques.(12,13) These derivatives may be set to zero, if no wing is used, or if only longitudinal stability is of interest for a winged aircraft. The roll and yaw moment of the wing is computed by:

$$t^* = \frac{b_w}{2V}$$

$$L_w = \frac{\rho}{2}S_w V^2 b_w \left[\left(XWG12 + XWG13\ C_{L_w}\right)\beta_f + \left(XWG14\ C_L r + XWG15\ p\right)t^*\right]$$

$$N_w = \frac{\rho}{2}S_w V^2 b_w \left\{\left[XWG16 + XWG17\ C_L{}^2\right]\beta_f + \left\{\left[XWG18\ C_L{}^2 + XWG19\frac{dC_D}{d\alpha}\right]r + \left[XWG20\ C_L + XWG21\left(YWG12 + 2\ YWG13\ \alpha_w \frac{AR_w}{AR_w + 3}\right).01745\right]p\right\}t^*\right\}$$

The effect of the rotor downwash on the wing is represented by adding the induced velocity of the rotor to the Z- and X-component of velocity which is used to determine the wing angle of attack. The calculated value of induced velocity is multiplied by the number input on the data cards and is assumed to act parallel to the mast.

Wing downwash and dynamic pressure reduction in the wake is represented by the following equations. The deflection of the wing wake, in the direction opposite to lift is given by:

$$\varepsilon_w = XWG09\ C_{L_w}$$

The dynamic pressure reduction along the wake centerline is:

$$\eta_{q_{max}} = \frac{XWG10\sqrt{C_D}}{\xi + .3} \cos^2\left(\frac{\pi D}{2h}\right)$$

where D is the distance from the wing trailing edge to the elevator leading edge in wing chords, h is the half-width of the wing wake at a point ξ wing chords down the wake centerline. The wingspan and chord are not input directly but are calculated from the input values of area and aspect ratio as follows:

$$c_w = \sqrt{\frac{S_w}{AR_w}}$$

$$b_w = \sqrt{AR_w S_w}$$

When no wing is used, c_w and b_w are set to urity for purposes of defining t^* which is used to nondimensionalize time in the stability section of the program.

2. Horizontal Stabilizer

The geometric and aerodynamic specifications of the horizontal stabilizer are similar to those of the wing although elevator wake calculations are not made. Four coefficients are currently used to represent the effects of the wing and rotor wake on the elevator. XEL11 is used to multiply the wing lift coefficient and the product represents the downwash angle at the elevator caused by wing lift. The rotor induced velocity is added to the Z-component of elevator velocity, after multiplication by a constant, in the same way as described previously for the wing. The constant is zero below the forward speed input in XEL09 and is equal to XEL08 above the forward speed input in XEL10. Between these two speeds, the induced velocity effect increases linearly.

For helicopters with a single main rotor, the speeds usually used are zero and one knot so that the elevator is always in the rotor downwash. For a helicopter like the XV-3, or other configurations which use laterally-disposed rotors, the velocities used depend upon wake skew angles and the location of the elevator. The multiplying factor usually used is two, since the induced velocity which is computed is considered at the rotor disk.

3. Vertical Stabilizer

The primary geometric and aerodynamic data used to describe the vertical stabilizer characteristics are similar to those described previously for the wing. Two aerodynamic interference effects are simulated: tail rotor induced velocity and the rate of change of fin angle of attack with sideslip ($\partial\sigma/\partial\beta$ in conventional terminology).

The tail rotor induced velocity is multiplied by XFN06 and added to the sideward velocity component of the free stream velocity vector acting on the vertical stabilizer. The tail rotor mast is assumed to be perpendicular to the X-Z plane of the aircraft. If the vertical stabilizer is to the right of a tail rotor which is providing a thrust to the right ("above" the rotor), then XFN06 is usually about 0.5. If the vertical stabilizer is to the left, then XFN06 is usually about 1.5, depending upon proximity of the fin and tail rotor.

The free stream velocity vector is modified further by the sidewash coefficient. The lateral velocity at the fin is given by:

$$V_{y_{fin}} = V_{y_{body}} (1 - XFN07)$$

If no sidewash effect is desired, then XFN07 is set to zero. Most single rotor helicopters have a value of about 0.2 for XFN07.

E. JETS

Auxiliary propulsion may be added in any specified amount by means of the input data of the jet group. Either one or two jets may be used.

The location of the right jet is specified as well as the pitch and yaw angle with respect to the body axis system. The left jet is assumed to be at the same station and water line and pitch angle. The buttline and yaw angle of the left jet are assumed to be the negative of the right jet. If only one jet is used, it is assumed to be the "right" jet and a negative buttline must be used if it is desired to locate the jet on the left side of the fuselage. The magnitude of jet thrust does not vary with speed in the current program. If no jets are used, the number of jets (XJET01) is set to zero.

F. CONTROL SYSTEM

The synthesis of the control system of a specified aircraft configuration is complicated because of the generality of the

mathematical model. The reader is referred to Volume II for a detailed discussion of synthesis of the control system.

The usual control system linkages used for three typical configurations are indicated in Table IX by x's. The controlled elements are:

- Incidence of aerodynamic surfaces:

  Horizontal stabilizer
  Vertical stabilizer
  Right wing panel
  Left wing panel

- Main (forward, right) rotor pitch controls:

  Collective
  Longitudinal cyclic
  Lateral cyclic

- Tail (aft, left) rotor pitch controls:

  Collective
  Longitudinal cyclic
  Lateral cyclic

- Auxiliary thrust:

  Magnitude
  Direction

These elements are controlled by the pilot or by automatic systems. The pilot controls used are:

- Collective pitch lever
- Longitudinal cyclic pitch stick
- Lateral cyclic pitch stick
- Pedals
- Mast conversion angle lever

The automatic systems simulated include a rotor speed governor, a bobweight, a flat tracker mechanism, and focused pylon geometry. The flat tracker equations provide cyclic inputs which act in such a way as to minimize rotor flapping. The focused pylon equations change cyclic pitch proportional to the rotor in-plane (H and Y) forces.

G. FLIGHT PATH EQUATIONS OF MOTION

The derivation of the equations of motion of the aircraft is given in matrix and vector form in Reference 4. No small angle assumptions are made in the analysis. Euler angles[12] are used to orient the aircraft with respect to the fixed reference system. Euler angle matrix transformations are used to transform positions, velocities, and accelerations from one axis system to another as required.

The center of gravity , gross weight, mass moments, and products of inertia are assumed in this analysis to include rotor mast and rotor blade weights. The change in center of gravity with mast conversion angle and with blade fold angle is accurately represented.

The rotors are assumed to be coupled together at a fixed gearing ratio. This enables the drive system to be approximated by one equation involving drive system inertia, supplied torque, and required torque. The rotor moments about the flapping hinge are resolved into sine and cosine components of azimuth position. These components then determine the resulting angular accelerations in pitch and roll of the rotor disk.

A summary of the equations is given in Table X.

SECTION IV

DETERMINATION OF THE TRIM CONDITION

This section of the report describes some of the pertinent details of the method used to compute the specified trim flight condition. The trim solution of the equations must be determined before any of the other capabilities of the program can be used. The trim solution becomes increasingly difficult as higher flight speeds and/or load conditions are attempted. The reason for this is that the terms in the equations of motion become more nonlinear as the effects of stall, compressibility, and reverse flow become more predominant.

A. MATHEMATICAL TECHNIQUE

There are ten equations which must be satisfied by the trim subroutine. The six equations of aircraft forces and moments (X,Y,Z,L,M, and N) are presented in Table X. The rotor moments are balanced by summing the contributions of all blades and then setting sine and cosine components of the following equation to zero for each rotor. The equation below is obtained by rearrangement of the blade flapping equation on page 28. The flapping positions and velocities which satisfy this equation then determine the rotor forces and moments.

$$\ddot{\beta}_J + \Omega^2 (\cos\beta + \eta) \sin\beta = 0$$

The trim solution is obtained by changing the values of the ten variables whose values are unknown and which affect the above equations. These variables are the four pilot controls, the longitudinal and lateral flapping angles on both rotors, the Euler pitch angle, and the tenth variable is either the Euler yaw angle or roll angle. The initial estimates of these variables which are part of the input data (the Flight Constants Group, XFC) must be reasonably close to the final values in order for the trim solution procedure to work. For normal, level-flight trim conditions, it is recommended to specify all pilot controls at 50%, all flapping angles and Euler yaw or roll angle at zero, and use some reasonable pitch attitude depending upon the configuration and speed. The values of the ten variables which are specified in the input data are then used in the mathematical model to evaluate the aerodynamic forces and moments. If the error between the desired and computed forces and moments exceeds the allowable values specified in the Allowable Error Group, XER, then changes must be made to the values of the variables so as to reduce the error.

In order to compute the amount of the changes, the effect of each variable on the ten equations is evaluated separately. This is done by incrementing each variable by a small amount (which is determined by the data supplied in the Iteration Limits Group, XIT) and computing the resulting changes in the forces and moments. These changes are then divided by the amount of the increment of the variable and the quotient represents the partial derivative. Mathematically, this procedure is expressed as follows. Let the equations (i) be represented by F and the variables (j) by x, thus

$$F_i = f(x_j) \qquad \text{where } i,j = 1 \text{ to } 10$$

For the increment to the jth variable, the ith equation can be represented as the sum of the un-incremented F_i and the change in F_i.

$$F_i + \Delta F_i = f(x_1 \quad x_2 \ldots x_j + \Delta x_j, \ldots x_{10})$$

The partial derivative is then

$$\frac{\partial F_i}{\partial x_j} = \frac{\Delta F_i}{\Delta x_j}$$

There are 100 partial derivatives evaluated and they are arranged in the form of a 10x10 matrix. When the errors in forces and moments are determined, these ten simultaneous equations are solved for the changes in the variables which are required. Checks are then made to make sure that the magnitudes of the computed changes are not too large. The new values of the variables are calculated by adding the computed changes to the values used in the last iteration.

The forces and moments are recomputed and a new partial derivative matrix is determined about the new trim point. If the equations were perfectly linear, there would be no change in the partial derivative matrix between iterations and only one iteration would be required. This is rarely the case, however, because of the nonlinear character of the rotor equations and aerodynamic surfaces which are stalled. An option is available to the user which reduces the computer time required to trim in linear flight regimes or when fairly small changes are being made by the sweep feature of the program. This option is specified by a non-zero input in XIT3 which then causes the program to recompute the partial derivative matrix on every fifth iteration.

B. CONVERGENCE

The above described procedure usually converges to a trim solution within 5 to 20 iterations. Usually, the maximum number of iterations allowed, XIT1, is 40. For some configurations and flight conditions, it may be difficult for the above technique to obtain the trim solution because of the nonlinearity of the variables. Mathematical science in the area of solution of nonlinear, simultaneous equations has not advanced to the point where solutions can always be found. In fact, most techniques will fail to converge unless the initial value is quite close to the final solution.

There are many reasons why the computer program may fail to converge to a trim solution. Because of the complexity of the program as well as the mathematical difficulties described above, it is not possible to determine a list of causes and cures which will always enable a trim solution to be found. The first check to make if trim is not obtained is to review all of the input values for keypunch or data errors. Described below are some of the more common sources of trim difficulties and the methods for getting a trim solution.

1. Iterative Repetition

Some cases will use all of the allowed number of iterations and still fail to trim. For these cases, the last sets of iteration data should be compared to each other to see if the same trim point is being computed every other (or every 3rd, 4th, etc.) time. To determine whether or not this is true, the values of the solution variables (VAR(I), I = 1 to 10) are compared to see if they are all equal. The most common causes of this problem are induced velocity or airfoil stall. The values of X-, Y-, and Z- force and L-, M-, and N- moment should be examined at each iteration to determine the magnitude of the force changes between trim conditions. The value of induced velocity should be examined for both rotors to see if changes are occurring between iterations which are large enough to induce force changes on adjacent aerodynamic surfaces that are a significant fraction of the total force change between iterations. For example, the change of wing load caused by a change in main rotor induced velocity or the interaction between tail rotor induced velocity and fin load. If this occurs, then the input data specifying the appropriate rotor wake effect may be in error or, if these data are correct, the damping term on induced velocity, XIT7, should be decreased. Normal values of XIT7 vary from 0.5 to 1.0 and may have to be decreased to 0.1 to 0.5 if this problem occurs. Sometimes a change of about 5 degrees of Euler angle about the appropriate axis will help get out of the induced velocity region where iterative repetition occurs. This may be tried if the above changes are unsuccessful.

Airfoil stall can cause iterative repetition if one trim condition results in unstalled flow on a fixed aerodynamic surface and the following trim condition results in stalled flow. The reason for this is the change in sign of the partial derivative of force with respect to angle of attack which is caused by the change in the slope of the lift curve at stall. If this occurs, the input Euler attitude angles can be changed about the appropriate axes to unstall the surface. If a high C_L condition is inherent to the flight condition being evaluated, the maximum C_L, YXX3, may be input at a larger than normal value in order to trim. The resulting C_L can be compared to a realistic value to determine the validity of the results. Another source of useful information about the above problems is the partial derivative matrix which should be computed and printed for every iteration if trouble is encountered in trimming the aircraft (XIT3 = 0). The values in the matrix should be compared from iteration to iteration to determine significant changes in magnitude and signs of the derivatives. Suspect derivatives can then be further traced back through use of the force and moment summaries to determine likely causes of the observed changes. This will often indicate what changes are required to obtain a trim solution.

2. Excessive Control Travel

For some cases, the iterative technique will result in one of the controls (VAR(I), I = 1 to 4) exceeding 100% or less than 0% travel. Trim may or may not be obtained in this instance. If trim is obtained, then an examination of the trim solution will usually indicate which aircraft parameters must be altered to bring the control travel into the normal range.

If trim is not obtained, then the force and moment summary data at each iteration should be examined to determine which elements are causing excessive forces and moments. The cause of the increase in the force or moment of the element should be isolated if possible. The partial derivative matrix should then be examined to determine which are the primary derivatives (indicated by largest numerical value) relating variables to the excessive force or moment. These variables should then be changed in the appropriate direction, indicated by the sign of the partial derivative, and then rerun the case.

3. First Iteration Technique

If the methods described above should fail to attain a trim condition, there is a method for enabling the user to better understand the dependency of the forces and moments on the initial values which are used in the input data.

The input values of allowable force and moment errors, XER1 to XER7, are set very large (9,000,000) so that the computer recognizes a "trim" solution no matter what the input data values are. All data are then printed out on both the iteration and trim page. Secondly, the sweep feature is used to enable the "trim" data to be computed for a suitable range of the input parameters which are specified by the sweep cards. The resulting variations in forces and moments with changes in the input variables are noted and a better approximation of the values of the variables for trim can be made. By using values which are closer to the trim condition, convergence of the computer program to the trim solution is more likely. A major advantage of this technique is the extremely short amount of time needed to compute data for one iteration.

SECTION V

DISCUSSION OF TYPICAL APPLICATIONS

The purpose of this section is to describe some of the more common applications of the computer program and to assist the user in gaining an appreciation of the effects of changes in the values of some of the input data on the computed flight characteristics. One of the major obstacles to the use of the computer program is the time and effort required to determine the values for over 400 items of input data. Once this is done, however, a powerful analytical tool is available which has extensive application during preliminary design, flight testing, and for investigating the effects of aircraft geometry changes, weapon recoil, external stores, and a variety of other parameters on the flight characteristics.

> It cannot be overemphasized that the quality of the results will never exceed the quality of the input data.

The mathematical model in the computer program is very realistic. If the input data define an unattainable flight condition because of physical laws or power limitations, then either no trim condition will be found or some aspect of the output data will not be realistic. The user must recognize this condition and correct the input data. Some of the input data require experience and judgment in the determination of values to use. These data are discussed below to assist the user in acquiring a working knowledge of the program.

A. PERFORMANCE CORRELATION

This is generally the first topic of interest after the initial values for input data have been determined from the geometric and physical characteristics of the aircraft. The extent of the correlation will be determined by the purpose of the subsequent investigations as well as the amount and reliability of data to which comparison will be made. Data measured in flight test will probably be best if they have been carefully measured and reduced. In the design phase of an aircraft, predictions made by the Aerodynamics or Performance Group are generally used.

1. Power Required

The total power required is computed for all trim flight conditions. The parameter sweep feature may be used to change gross weight, speed, and drag area, while using only one basic

set of input data. Drag area changes must often be considered because the configuration of external stores will change the effective drag area of the aircraft.

The major contributors to rotorcraft power required are:

- flat-plate drag area
- rotor induced power
- rotor profile power

There are several input data that have a first-order effect on the magnitude of each of the above terms. The magnitude of these terms varies with speed and weight in very different manners. These relationships will be reviewed to assist the user in determining which power contributor should be modified to improve correlation.

In the computer program, flat-plate drag area is divided into the following primary components.

Component	Input Data Specified
- fuselage	XFS22 through XFS25
- wing	XWG1 and YWG12 to YWG14
- elevator	XEL1 and YEL12 to YEL14
- fin	XFN1 and YFN12 to YFN14
- jets	XJET2 and XJET3
- rotor hub	XMR21 and XMR25

For initial performance work, the drag contribution of the above components is not as important as the total flat-plate drag. Reasonable estimates of drag coefficients and areas are adequate at this point. The effect of flat plate drag on power required is a velocity-cubed function. It is the product of the drag force and the velocity cubed.

$$P_f = 0.5\rho f V^3$$

Knowledge of this characteristic relationship is useful when making small corrections to the input data, above, in order to reduce power discrepancies which vary as V^3.

Rotor induced power is determined internally and is not subject to modification by altering input data values. Induced power can be approximated by the product of the rotor thrust, usually equal to the gross weight, and an induced velocity which is based upon momentum theory. This induced velocity is calculated by solving the following equation for V_p in an iterative manner.

$$V_p - \frac{P_f}{GW} = \frac{GW}{2\rho A\sqrt{V_p^2 + V^2}}$$

where P_f represents the flat plate drag power discussed previously.

Once V_p is determined, it is used in either side of the above equation which is equal to the induced velocity, i.e.,

$$V_i = V_p - \frac{P_f}{GW}$$

In hovering flight, it is apparent that the above equation for V_i reduces to

$$V_i = \sqrt{\frac{GW}{2\rho A}}$$

and in forward flight above about 60 knots, $V^2 >> V_p^2$, so

$$V_i \cong \frac{GW}{2\rho AV}$$

These approximate expressions are often adequate for correlation purposes. The actual induced velocity equations used are much more complex and account for spanwise variation and ground effect.

Rotor profile power is nearly constant but varies somewhat with thrust, or gross weight, as well as speed. The variation with speed, which is caused by flow asymmetry in forward flight, is inherent in the blade element representation of the rotor and is not subject to user modification by means of input data. The variation with thrust is also built into the rotor representation but may be modified by the user through the input data for the airfoil characteristics subroutine. The approximate effect on power of varying input data in the rotor aerodynamic group will be discussed below. The exact drag equation

used is described in Section IIIB and includes stall and compressibility effects.

Most of the rotor operates in the unstalled, subsonic flow regime. The drag coefficient equation for a main rotor blade element operating in this regime may be approximated by

$$C_D = YMR12 + \alpha(YMR13 + \alpha YMR14)$$

where α is the local section angle of attack. For purposes of overall correlation, an average value of α is needed. This value may be arrived at through the expression for C_L and the input YMR17. Since, for symmetrical airfoil sections, YMR13 should be zero, the following may then be used:

$$C_D = YMR12 + YMR14\left(\frac{7C_T}{\sigma YMR17}\right)^2$$

or, in dimensional terms, with YMR17 and YMR14 in consistent units,

$$C_D = YMR12 + YMR14\left(\frac{7GW}{\rho(YMR17)bcR(\Omega R)^2}\right)^2$$

where b is the number of blades. The profile power may then be approximated by:

$$P_0 = C_D\left(\frac{\sigma}{8}\right)\rho A(\Omega R)^3\left[1 + 4.6\left(\frac{V}{\Omega R}\right)^2\right]$$

The effectiveness of the inputs YMR12 and YMR14 on power required is apparent after substitution into the preceding two equations. The input values can then be adjusted within reasonable limits to improve power correlation with variation in speed and gross weight.

Power divergence is sometimes apparent in test data above a certain forward speed. This is caused by compressibility effects on drag. These effects also appear as different C_P-C_T curves with different rotor speeds. The input variable which affects the magnitude of compressibility effects is YMR1, the critical Mach number of the airfoil used. YTR1 affects tail rotor power in a similar manner. Typical values for YMR1 vary from .78 to .88 depending primarily on thickness.

2. Wing-Rotor Lift Sharing

One of two problems are generally considered in this regard. Either correlation is desired between measured and computed

data, or geometric and control system parameters are being optimized during the design phase to achieve a specified lift sharing ratio.

In the former case of correlation with measured data, only one input will directly alter lift sharing significantly. This input is XWG8 which multiplies the induced velocity of the main rotor and adds the resulting velocity vector, which acts along the mast, to the free stream velocity vector to obtain the wing angle of attack. Typical values of XWG8 are 1.0 to 2.0, depending upon wing location. Another significant factor is the variation of fuselage pitch attitude with forward speed, gross weight, center of gravity location, and external stores configuration. All inputs which have an effect on pitching moment equilibrium will affect the fuselage pitch attitude. Listing all of these inputs would take too long and be too dependent on the configuration to be valid. Also, many of the terms which affect pitching moment are determined by other considerations. Some of these terms are hub spring restraint, elevator incidence and location and gearing, and wing incidence and location. It is desired to find input values that can be altered within reasonable limits to improve correlation and values which do not have strong impact in other areas of the design. These inputs are usually the fuselage pitching moment coefficients, XFS15 and XFS16. Fuselage lift and drag characteristics and the location of the aerodynamic center may be altered somewhat, but these changes will significantly affect cyclic control stick margins and gradients as discussed in the subsequent section.

If the desired lift sharing characteristics are known for a specified design, the user has freedom to determine geometric and control system parameters in order to meet the desired lift schedule. As these parameters are changed, the effects on stability, control margins, control gradients, and power must also be considered. A combination of parameters that satisfies the lift schedule at the expense of violating one of the other areas mentioned is of little practical use.

If the wing has no movable surfaces or is not wholly movable, then the control system parameters will not have a first-order effect on lift sharing. If the wing incidence is variable, the effect of different combinations of changing incidence with collective pitch and/or longitudinal cyclic pitch may be determined by changing the appropriate inputs in the Controls Group, the XCON inputs. Geometric parameters of the wing that are usually altered to change the lift schedule are: area, XWG1; horizontal location, XWG2; incidence, XWG5; and to some extent, aspect ratio, YWG18. The first two of these parameters have a strong influence on

control margins, gradients, and aircraft stability so these effects must be examined concurrently with the lift-sharing schedule.

B. STABILITY AND CONTROL ANALYSIS

Control positions are determined for all trim flight conditions. The control power derivatives are also determined which relate the change of pitching, rolling, and yawing moment to control deflection. The stability analysis and vector analysis sections may also be used to determine the effects of parameter changes on the flying qualities of interest.

The computer program is usually used either to correlate measured data or to determine geometric and control system parameters of new aircraft designs. The user generally has more latitude in altering values of input data during design studies than for correlation studies of actual aircraft. Although this gives greater flexibility, it also increases the number of variables being considered, so care must be taken in selecting which variables to alter and in what combinations.

1. Control Margins and Gradients

After performance correlation is obtained, the control position and gradient variation with changes of airspeed, gross weight, center of gravity location, and external store configuration are then examined. If the correlation is not adequate, some of the input data may be adjusted within reasonable limits to improve correlation.

The amount of longitudinal cyclic control which is required to trim pitching moments will vary with forces and moments acting on the fuselage. The variables which affect this are the same as those which affect pitch attitude. In addition to these, the apportionment of drag area between the fuselage and the hub may be altered somewhat because of the uncertainty associated with determining an accurate, full-scale hub drag value. Re-proportioning the drag areas will change the pitching moment acting on the fuselage and result in a change in control stick position required to trim. The control power data are useful in determining how much of a change is required in pitching moment to move the control a specified amount. Since the total drag area does not change, the power correlation will not be affected significantly.

Lateral cyclic and pedal control required to trim will vary with forces and moments acting on the fuselage and fin. In the absence of wind-tunnel data, several variables may be

varied within reasonable limits because of the difficulty of measuring or estimating their effects precisely. These variables are:

- effective fin aspect ratio, YFN18
- effective fin area, XFN1
- fin aerodynamic center, XFN2 and XFN4
- sidewash coefficient, XFN7
- Fuselage yaw moment, XFS17 and XFS18
- Fuselage side force, XFS26 to XFS28
- Fuselage aerodynamic center, XFS2 and XFS4

Although data obtained in the wind tunnel are better than estimated data, exact correlation will probably not be achieved because of Reynolds Number effects and the effect of the actual rotor flow field impingement on the fuselage and aerodynamic surfaces. Some latitude may be used in the values assigned to the input variables to account for these effects.

2. Control System Kinematics

A wide variety of control system linkages may be synthesized by input data, as previously described in Section IIF and Table IX. This capability is especially useful when designing the control system of new aircraft. Elevator synchronization schedules with collective pitch, and longitudinal cyclic pitch and mast tilt may be altered by the inputs XCON11, XCON27, XCON28, XCON63 and XEL5. The corresponding changes in control margins and gradients are then computed for the specified configuration (weight, cg, external store) and flight condition (speed, load factor, altitude).

The tilt-rotor concept uses differential collective pitch for roll control in helicopter mode and differential longitudinal cyclic pitch for yaw control. As the rotors are converted through ninety degrees, these swashplate motions result in lateral cyclic control producing yaw motion and pedal control producing a roll motion unless some means of phasing these controls with conversion angle are used. In addition to this change of control response, the rotor cyclic and differential collective controls must be phased out so that only collective pitch is controlled by the pilot (or governor) in airplane mode. In order to investigate how these controls should be phased, the computer program was used to compute yaw and roll moment caused by pedal deflection with different

amounts of differential collective pitch being actuated by pedal motion. The results are summarized in Figure 6. It was desired to determine the coupling that would minimize the roll moment caused by pedal deflection while maintaining a linearly decreasing value of yaw control power. The dashed lines achieve these results at the design conversion speed if a 15° mast tilt is used above 80 to 100 knots. The resulting control kinematics are also shown in Figure 6. The effects of other control system linkages for other aircraft or helicopter configurations may be easily determined in a similar manner. Other topics of interest may include wing flap/aileron linkage, rudder-tail rotor lift-sharing, elevator synchronization, other control phasing with mast conversion, effects of governors and bobweights and other parameters.

3. Stability Characteristics

The stability derivatives are computed by the increment technique discussed in detail in Section IIB. The contributions of the various components of the aircraft to any stability derivative may be determined by examination of the output data as shown in Table I. The accuracy of the derivatives may be rapidly determined from the data available and by using the standard equations for the fuselage and fixed aerodynamic surfaces. The input parameters that alter these derivatives will be apparent to the fixed-wing aerodynamicist.

The rotor force and moment derivatives with respect to linear and angular rates will correlate well in low-speed flight with derivatives which are available in the literature.[15,16] In high-speed flight, the more accurate representation of the rotor in the computer program will compute more accurate stability derivatives. These derivatives will include the nonlinear effects of stall, reverse and radial flow, and compressibility which are not subject to simple, closed-form analysis.

The rotor derivatives may not be computed in the stability section if the relationship between the increment size, XIT4, used and the allowable error in rotor moment balance, XER6 and XER7, is not properly proportioned. The reason for this is that the rotor subroutine will only compute new flapping angles if the linear or angular rates cause a change in flapping moment that exceeds the allowable error in flapping moment. If the rate changes are too small or if the allowable moments are too high, then no change in flapping will occur because of rates, and the rotor force and moment derivatives will be zero. This condition is illustrated in Figure 2 where the increment size, XIT4, is below a value of 0.04; that is, the change in linear velocities is 0.4 feet per second and the change in angular velocities is 0.004 radians per second. The usual value of XER6 that is used is 50 pound-feet, which was the

value used in this 140 knot sample case. A velocity increment of 0.4 feet per second perpendicular to the 140 knot velocity vector will induce an angle of attack or side-slip change of only .0017 radians. This small a change is insufficient to cause the program to rebalance the flapping moment. It should also be noted that for very low increment sizes the resulting small differences of large numbers will cause a wide variance in the values of the computed derivatives. A good rule of thumb for the increment size to use in the stability analysis is XIT4 = 0.002V, where V is in feet per second. For the sample case of Figure 2, XIT4 should be 0.5.

If the program is being used for correlation with measured data, relatively few inputs may be changed to improve correlation. Experience indicates that correlation between measured and computed frequencies and damping characteristics is good, and the input data seldom needs changing if the initial values were carefully determined. Errors in input data can often be traced back by means of the stability analysis section which provides the user with data concerning the contribution of each element to a stability derivative. Some of the more important input data in this regard are those which account for aerodynamic interference effects. These data are:

- XWG8 — Main rotor wake on wing
- XWG9, XWG10 — Wing wake on horizontal stabilizer, η_q
- XEL8 — Main rotor wake on elevator
- XEL9, XEL10 — Variation of XEL8 with forward speed
- XEL11 — Wing wake on horizontal stabilizer, $d\varepsilon/d\alpha$
- XFN6 — Tail rotor wake on fin
- XFN7 — Fin sidewash caused by fuselage and wing

The program may be used to compare the stability characteristics of a new aircraft to requirements and then change appropriate design parameters if the requirements are not met. In this case, best approximations of the above interference effects should be made based upon the specific configuration. Since the rotor induced velocity is computed at the disk, the coefficient to use to simulate an airfoil in a fully developed rotor wake is 2.0, but values of 0.5 to 1.0 are more representative of actual flow conditions. The flow angularity, XEL 11 and XFN7, at the empennage which is caused by the wing may be estimated by conventional methods (12,13,16) if wind tunnel data are not available.

The input parameters most commonly varied to study control-fixed stability are those relating to the size, incidence,

aspect ratio, and placement of the fixed aerodynamic surfaces. The sweep technique discussed in Section IIA enables the effect of changes of these parameters on stability to be easily determined. The computed frequency and damping characteristics enable direct comparisons with specification requirements to be made. Since trim flight data may be obtained in climbing and descending flight, the effect of power on control position may be directly determined. The neutral point may be determined by computing stability derivatives as the center of gravity, XFS5, is moved aft. The cg location at which the change of pitching moment with angle of attack, $dM/d\alpha$, is zero is the neutral point. The maneuver margin may be determined in a similar manner by examining the change in the longitudinal cyclic pitch required to trim as the cg is moved. The cg location for which the longitudinal cyclic pitch does not change as the cg is moved determines the maneuver point.

Many other applications of the program to stability and control investigations are possible. The examples given above are intended to be illustrative and not exhaustive.

C. MANEUVERING FLIGHT

The maneuver computing section of the program is used to graphically illustrate the control and gust response characteristics of the aircraft. Many flying qualities specifications are expressed in terms of a range of acceptable deviations of certain parameters during the performance of a maneuver. Although this type of specification is intended primarily for application in flight test, the maneuver computing section of the program enables the maneuver to be simulated to determine specification compliance. The effect of design parameters on the response may be evaluated for new designs, or the computed and measured maneuver time histories may be compared. If the measured response is not acceptable, the computer program may be used to investigate different ways of obtaining acceptable response.

1. Nonlinear Effects

Since the equations of the maneuver section of the program are fully coupled and nonlinear, response to simultaneous longitudinal and lateral control or gusts may be computed. The vector analysis section can be used to represent as a vector quantity any parameter that can be plotted. The magnitudes and phase angles of the vectors can then be compared to the mode shapes computed in the stability analysis section. If the vector relationships and mode shapes are about equal, as they usually are, then the nonlinear effects are small

and the data obtained in the linear, uncoupled stability section accurately represents the stability characteristics.

The correlation between these methods is not automatically assured. Although the mathematical model is the same, the techniques used to compute stability are quite different. The stability section uses the computed stability derivatives in linear perturbation equations and then computes the roots of the characteristic equation. The maneuver section continuously extrapolates to the next maneuver time point by applying the Runge-Kutta technique (described in Section IIC) to the differential equations of motion of the aircraft, a partial list of which is in Table X.

The data in the stability section are usually computed in less than a minute on the IBM 360, Model 65 computer. Maneuver cases take approximately one minute of computing time per second of maneuver time. This restricts most maneuver investigations to short period phenomena and encourages the use of the stability section method, since most flight conditions are characterized by linear response.

2. Rotor Flapping

The stability section computes the rotor derivatives with respect to flapping, but no information is provided concerning flapping response to control motion or gust penetration. The maneuver section is well suited to this type of work because the high frequency and damping of flapping motion require a relatively short maneuver time.

The amount of rotor flapping freedom that must be provided in both accelerated and unaccelerated flight may be determined from the data computed in the trim section. During a rotor design study, many flight conditions are examined which determine different parameters of the aircraft. Once the flight conditions which exhibit the larger flapping angles have been determined, the maneuver section is used to compute the flapping resulting from control motions and gust penetration in the direction which tends to increase flapping.

For rotors with no flapping freedom, the mathematical model provides for a nonisentropic hub spring of specified stiffness (XMR17 and XMR18) which is located at a specified radial location (XMR16). The hub moment of a "rigid" rotor is then indicated by the product of the computed flapping angle and the hub restraint. Changes in design parameters may be made in the input data, and the effects on flapping will be computed for the design flight conditions. In the event that unacceptable flapping angles or hub moments are computed, suitable changes must be made in the design to reduce flapping.

Some of the more effective parameters which reduce flapping in maneuvering flight are those which reduce rotor blade loading (increased chord or radius) or reduce the amount of thrust change required from the rotor in order to attain a specified normal acceleration. Although a wing is effective in altering the latter, the size must not be so large as to unload the rotor in autorotation (loss of rotor speed control) or require too great a change in the longitudinal cyclic pitch required to trim pitching moments caused by power changes.

3. Response Characteristics

Two types of response are generally of interest: control response and gust response. There are several different shapes of gusts that may be simulated in the computer program as described previously in Section IIC. This section will discuss some of the techniques used when investigating response characteristics.

Some aircraft exhibit strong coupling between pitching, rolling, and yawing motion because of the inherent configuration of the aircraft or because of the flight condition. It is often desirable to study the effects of design parameters on response about one axis at a time or about one pair of axes at a time. This is easily simulated in the computer program by increasing the inertia about the axes about which no motion is desired. A typical value for these inputs (XFS8 to XFS10) to lock out motion would be 9,000,000 slug-feet^2.

When the program is used to compute the response to control inputs, some care must be exercised not to use step inputs. Not only are step inputs impossible to attain in practice, they also cause a divergent oscillation to occur in the time-variant solution of the differential equations of motion. This divergence would not occur on an aircraft, but is caused by the inability of the Runge-Kutta technique to accurately represent step changes of parameters. When pilots are requested to make "rapid" or "step" control inputs, they usually use from 0.15 to 0.20 seconds to make the control motion. At least this amount of time should be used to make control position changes in the maneuver section.

If a step input must be made, it can be effectively simulated by using a very small control input duration, on the order of 0.001 seconds, and a time increment (Δt = 0.0001 seconds) which results in at least ten control increments to accomplish the input. This method is as effective as a step input, and avoids the divergence resulting from a large step change in the mathematical model.

4. Conversion Maneuvers

The user must specify the position of all pilot controls during the computation of maneuver response characteristics. Before a conversion maneuver can be computed then, the required control positions must be known in advance. This may be done by computing trim flight conditions for partial conversion configurations and then using the control position versus conversion relationship to determine the required time dependent control positions during the conversion maneuver. For example, consider the TFTA aircraft operating in helicopter mode with rotor masts vertical. The parameter sweep feature can be used to determine the trim control positions at 15, 30, 45, 60, 75, and 90 degrees of rotor mast conversion angle at the same airspeed. After these data have been computed, they can be plotted as a function of time once the user specifies the conversion angle versus time relationship. The resulting time histories of control motion can then be approximated by a series of control rates and time durations and then input to the maneuver section on appropriate "J" cards (Vol. II, p. 60).

This same technique can be used during rotor stopping by computing trim conditions at different rotor speeds as well as rotor blade fold angles. Care must be used to insure that all pilot controls have effective control power even at reduced and zero rotor speed. Not only is this required in an actual aircraft, the partial derivative matrix in the trim section will be singular if this condition is not met by the control system linkage specified by the input data. This usually means that the "fixed wing" control surfaces must be active before the rotor is stopped and folded.

Stopping the TFTA rotor is done most easily by reducing the power supplied (J = 13 card) and by increasing the collective pitch of the rotors (J = 1 card) to the feathered position. The high pitch setting required to feather (i.e., zero torque at zero RPM) the rotor can be approximated by computing the collective pitch required to set the angle of attack at the 0.75 blade radius equal to zero. Depending upon the rotor hub design, the rotor speeds at which the flapping stops (J = 28 card) are activated and/or the hub spring rate (J = 23 card) is changed, must be specified. If the rotor must be stopped at a specified azimuth location, a rotor brake must be simulated (J = 18 card). Once stopped, the TFTA rotor blades are folded aft uniformly (J = 6 card). Any control motions required during this maneuver must also be specified by appropriate "J" cards.

Stopping the HSF rotor requires use of the "J" cards mentioned above except that the J = 27 card is used to fold the blades

instead of the J = 6 card. Prior to stopping the rotor, the trim flight condition must be determined which results in rotor thrust and flapping near zero. This condition minimizes loads and angular motions of the aircraft during the stopping and folding maneuver. Once the rotor is stopped, the blade azimuth position of each blade must be specified as a function of time by use of as many J = 27 cards as required to define the relationship. Blade feathering positions during the fold cycle continue to be related to the rotor control positions by means of the sine and cosine functions of the azimuth angle as well as the collective pitch. Minimizing rolling and pitching moments during the fold cycle currently requires several trials with high fuselage inertias which use different rotor control relationships for each trial.

SECTION VI
CONCLUSIONS

The analysis techniques described herein provide a versatile and powerful tool which can provide data concerning performance, stability and control, blade airloads, and maneuvering flight in one integrated computer program.

The addition of equations representing the stop-fold rotor aircraft in the mathematical model enables accurate computation of the characteristics of this concept. Both the horizontal-stop-fold rotor and the tilt-forward-trail-aft rotor characteristics may be determined.

The generality of the mathematical model of the computer program enables the user to simulate fixed-wing as well as rotary-wing aircraft. The former may be jet or propeller driven and the latter may utilize single, tandem, or side-by-side rotor configurations. The generality of the program requires over 400 values to be assigned to input data to completely describe the aircraft being simulated.

The maneuver simulation enables the effect of changes of design parameters to be determined. Flying qualities specifications which are written assuming determination of compliance by flight test may be examined by simulating the required maneuver with the computer program.

Aerodynamic interference effects are significant to the accurate evaluation of stability and control characteristics and have been included in the computer program. Nonlinear aerodynamic characteristics can adversely affect the ability of the computer program to compute the trim flight condition.

The consistent use of vector algebra and the complete matrix form of angular rotations eliminates all small angle assumptions in the analysis.

It is recommended that this computer program be developed further to:

- increase the sophistication of the mathematical model
- provide additional output data in more convenient form
- include aeroelastic blade loads if computer size permits
- include additional equations describing automatic stabilization functions
- compute linear, coupled stability characteristics
- represent control-free stability characteristics directly

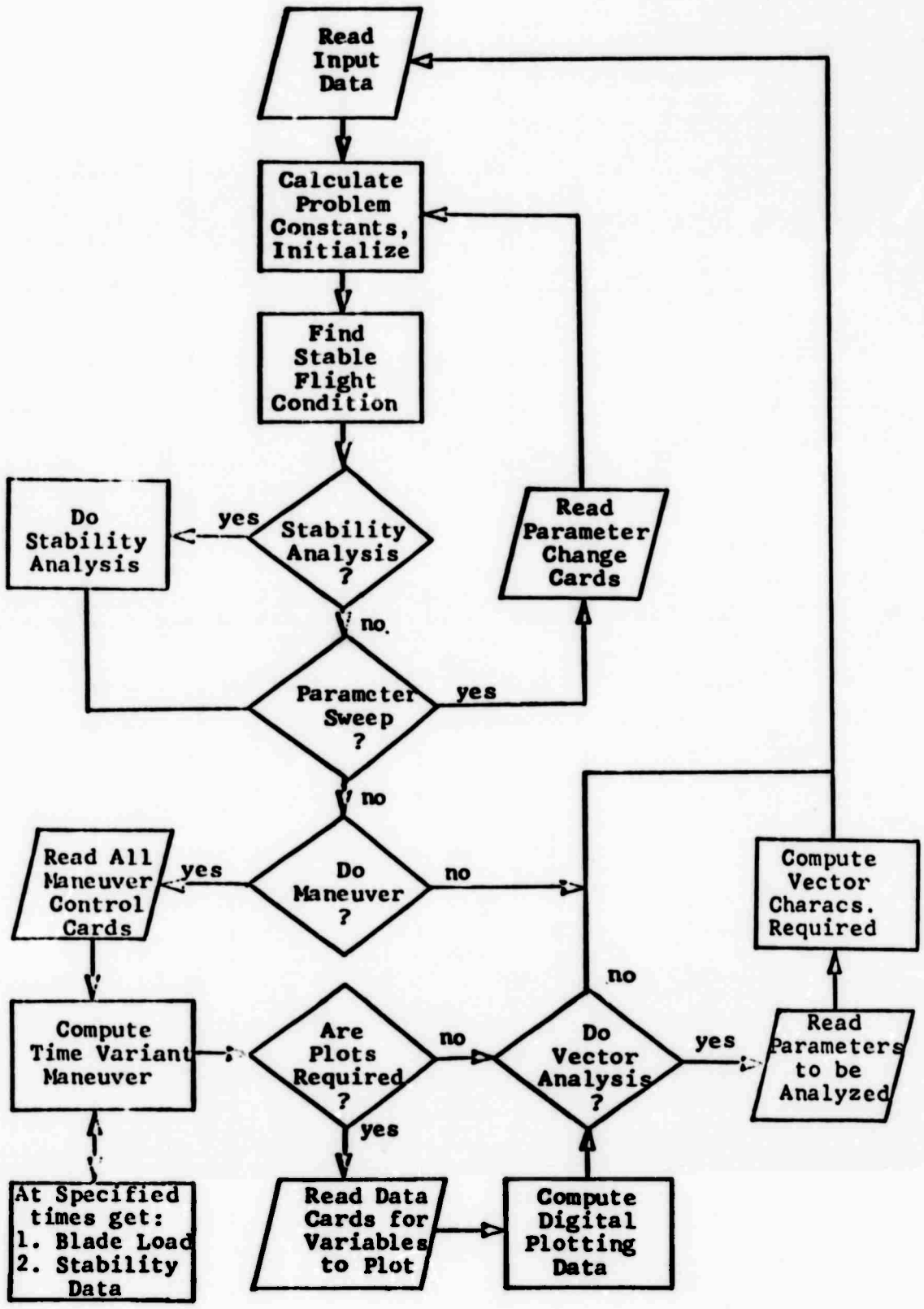

Figure 1.- Major Computational Functions Flow Chart

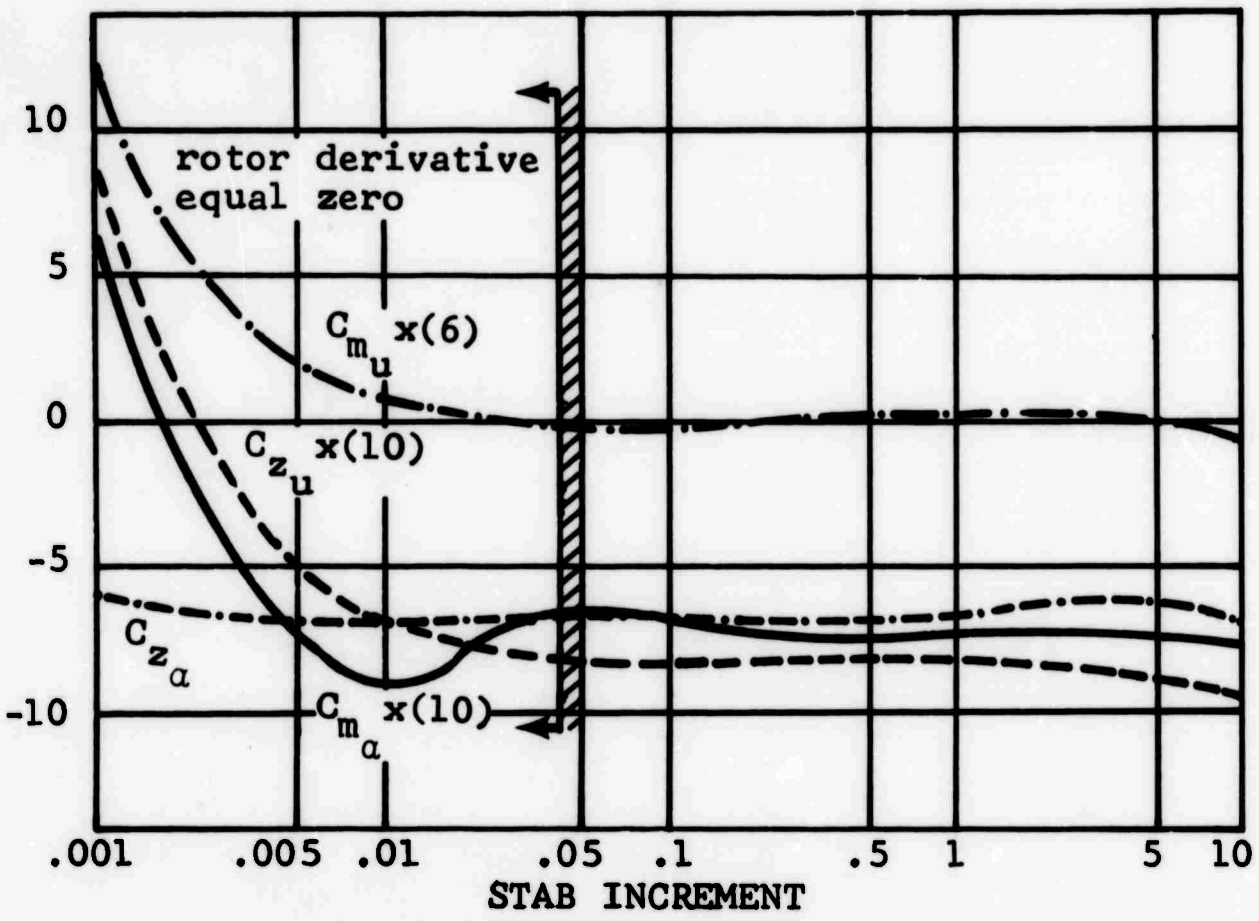

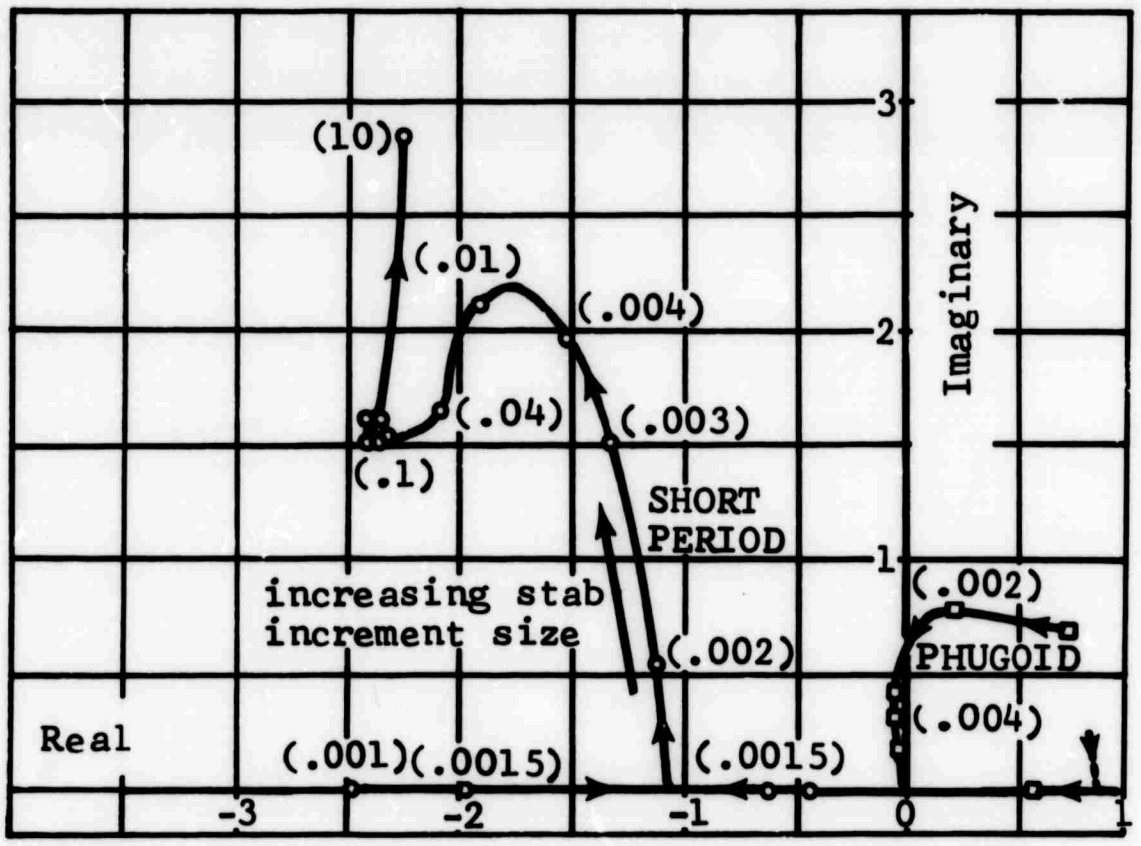

Figure 2. The Effect of Increment Size on Stability Derivatives

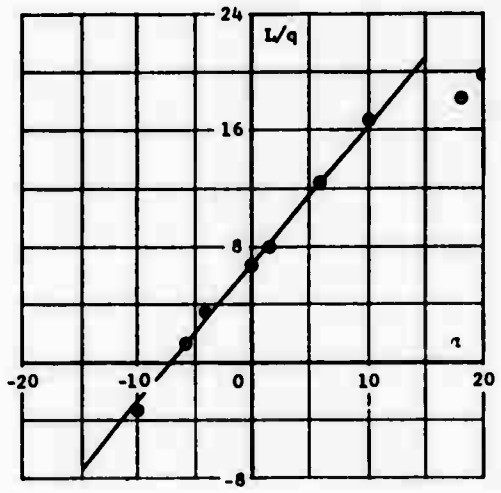

$L/q = (6.7 + 0.95\alpha)(MS)^2$

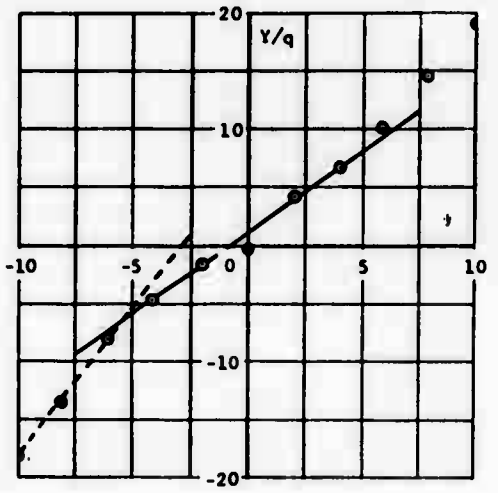

$Y/q = (1.1 + 1.4\alpha)(MS)^2$

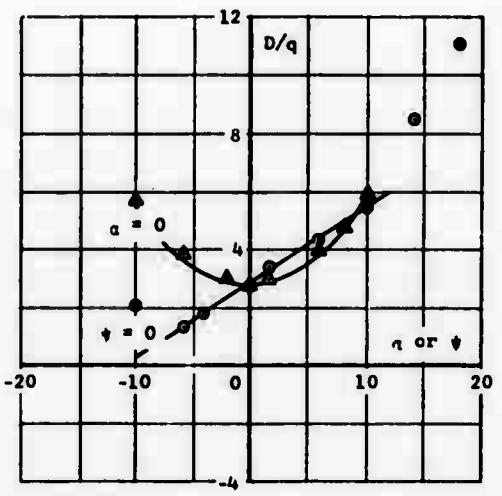

$D/q = (2.85 + 0.27\alpha + 0.295\psi^2)(MS)^2$

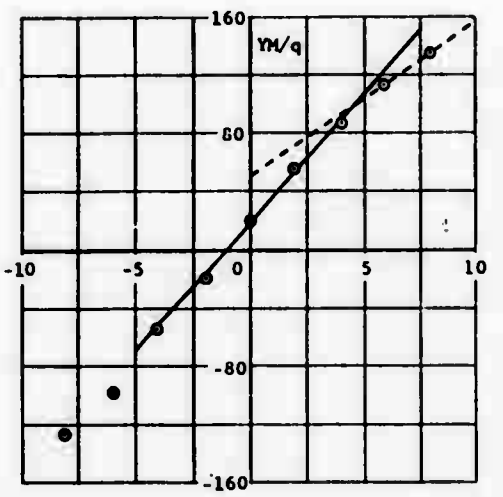

$YM/q = (18.0 + 17.7\alpha)(MS)^3$

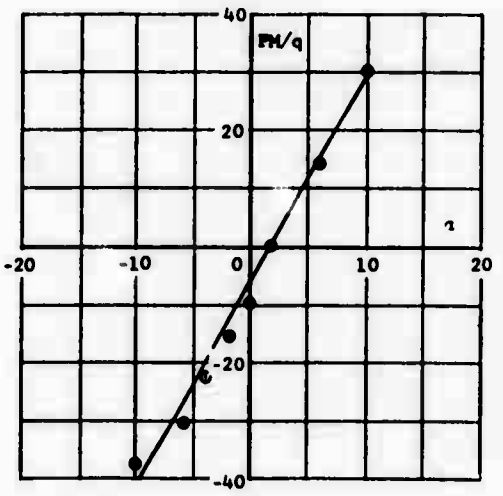

$PM/q = (-6.0 + 3.5\alpha)(MS)^3$

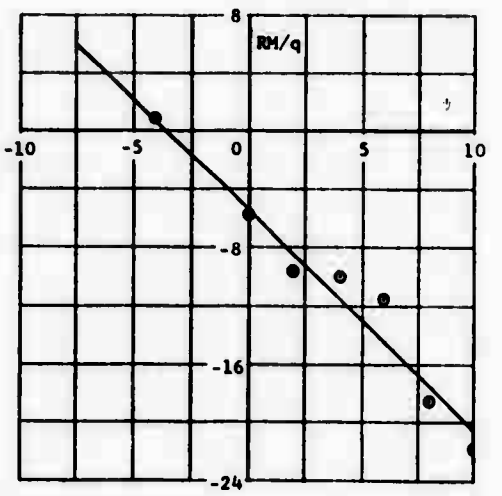

$\Delta WL = (12)(MS)\frac{\partial(RM/q)/\partial\psi}{\partial(Y/q)/\partial\psi}$

MS = 1/MODEL SCALE

Figure 3. Wind Tunnel Data for a Helicopter Fuselage

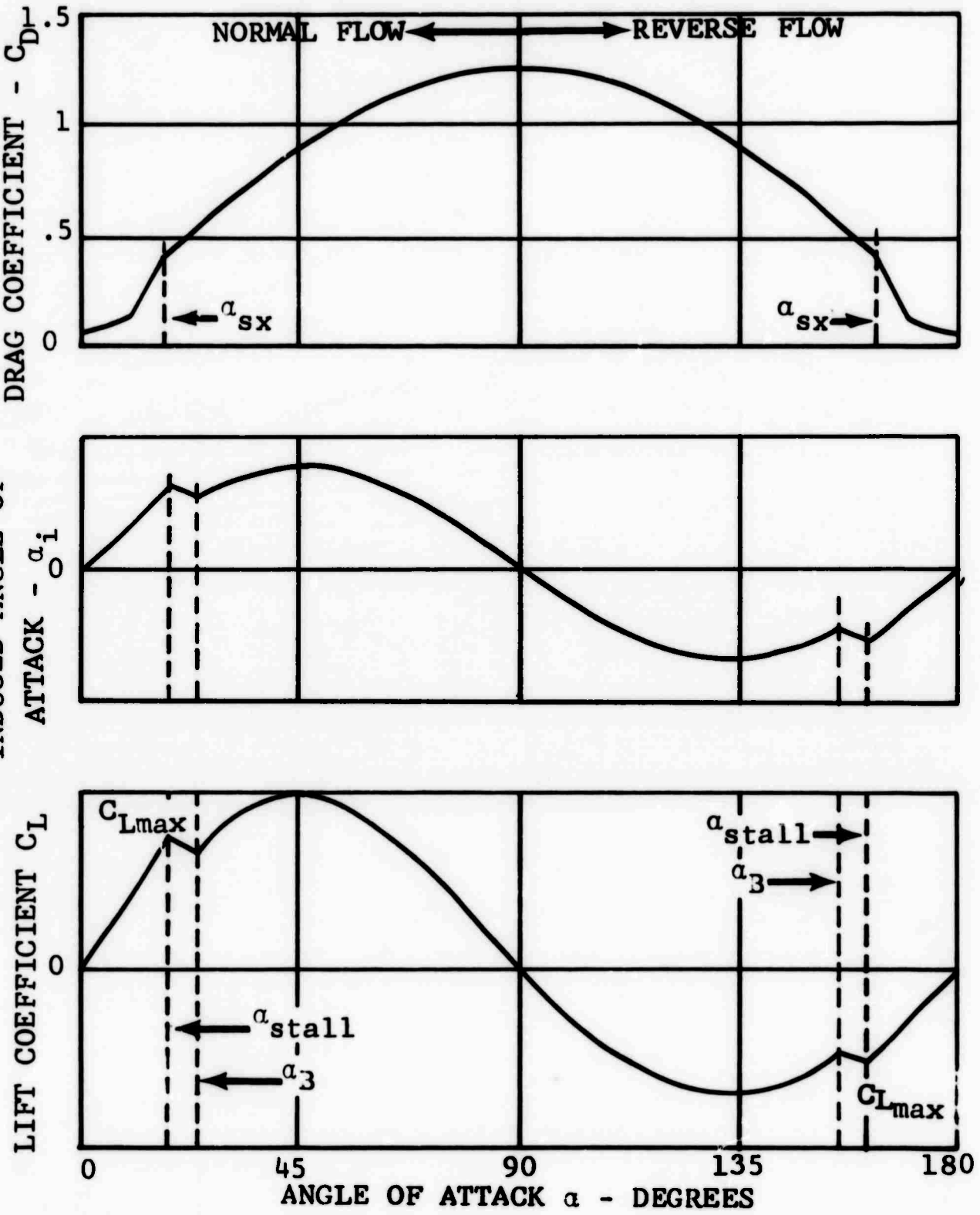

Figure 4. Typical Airfoil Characteristics Data

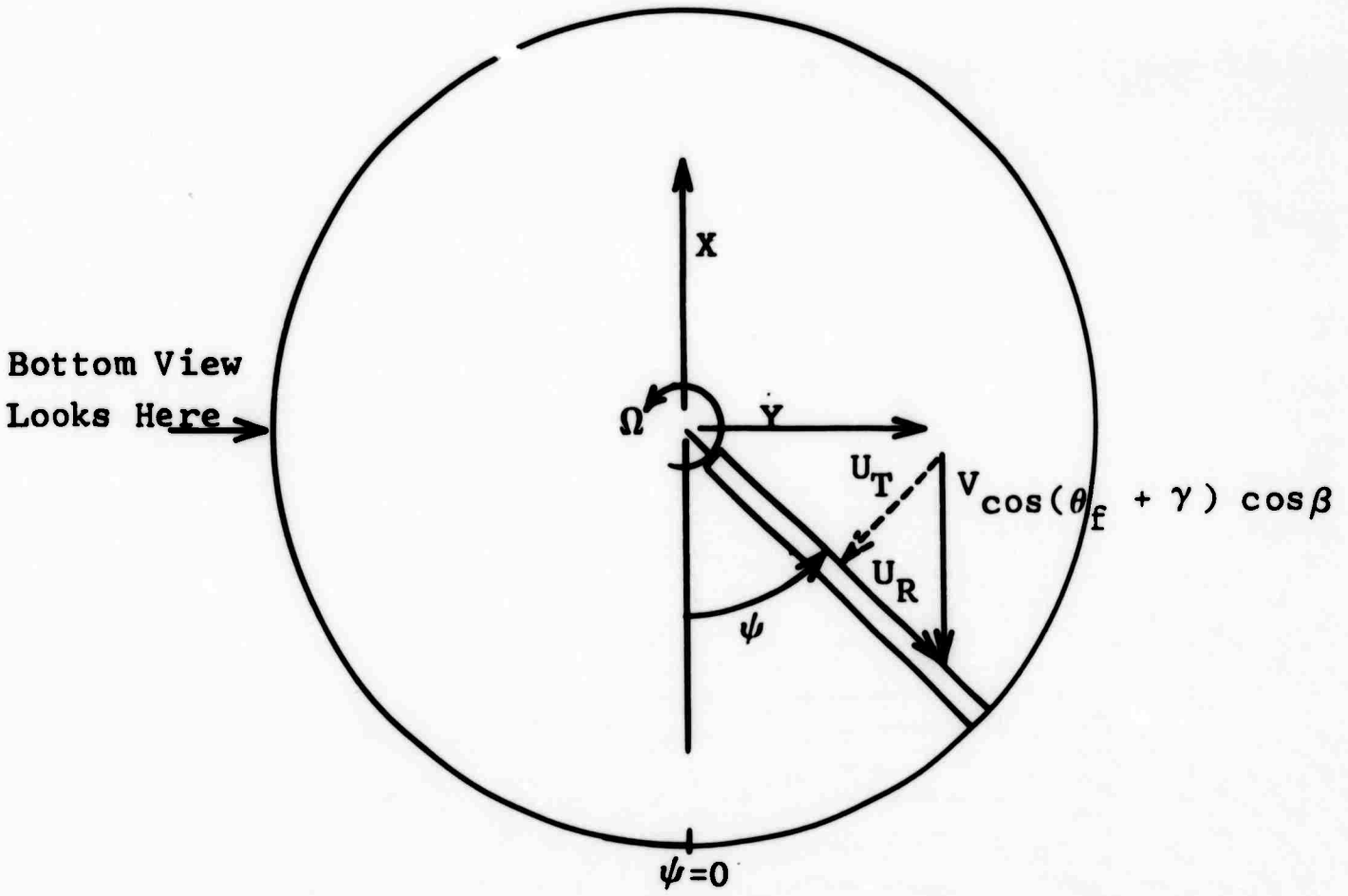

Figure 5. Velocity Resolution at a Blade Element

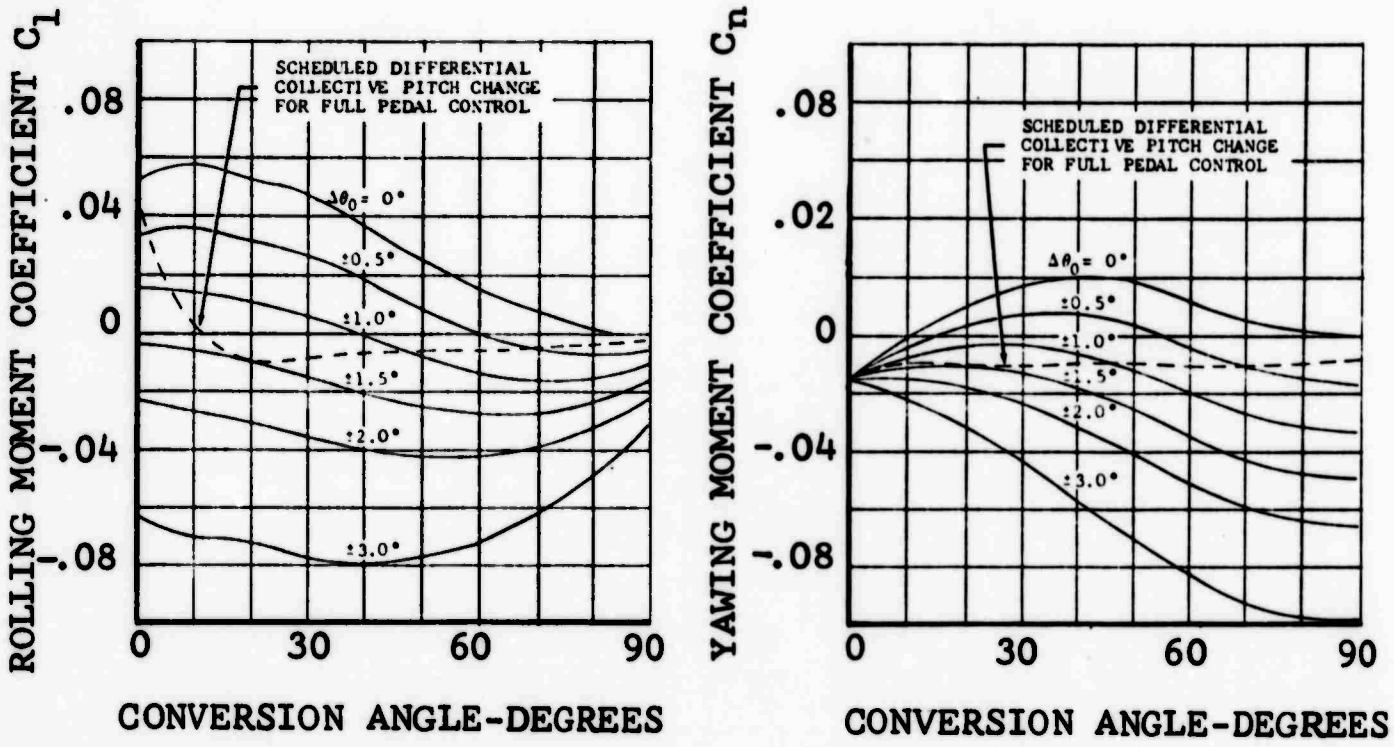

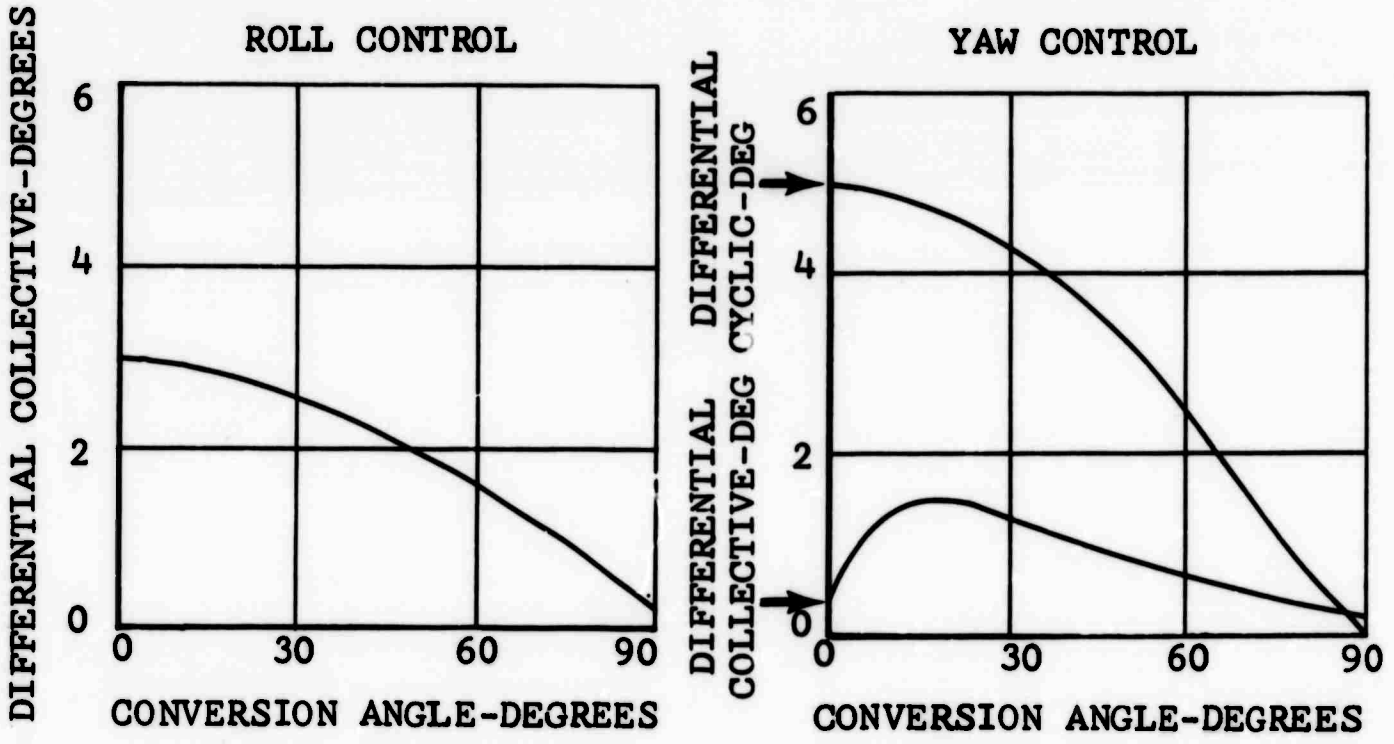

DIFFERENTIAL CYCLIC OR COLLECTIVE PITCH CHANGE RELATIONSHIPS FOR FULL CONTROL TRAVEL

Figure 6. Control System Phasing

TABLE I

STABILITY SUBROUTINE OUTPUT DATA

***** START OF ITERATION 9 *****

VARII 27.11028 49.37386 57.72380 31.11125 -8.40972 29.89423 4.43068 1.07340 1.66202 0.23574

	THRUST	H-FORCE	Y-FORCE	TORQUE	IND. V.	CONING	JET THRUST	
MAIN ROTOR	9760.	878.	12.	11861.	7.423	2.234	RIGHT/CENTER	0.
TAIL ROTOR	285.	16.	6.	37.	5.787	1.490	LEFT	0.

FORCE AND MOMENT SUMMARY

	TOTAL	R.WING	L.WING	ELE	FUS	R.JET	L.JET	M.R.	T.R.	GUN	FIN	W/OMR	QTR
X-FORCE	-0.1	-46.7	-46.7	13.2	-159.3	0.0	0.0	-878.1	-15.5	0.0	-22.4	1155.4	
Y-FORCE	5135.9				685.6	0.0	0.0	12.2	284.5	0.0	258.5	3895.0	
Z-FORCE	-2955.5	-176.6	-176.6	155.2	221.3	0.0	0.0	-9760.6	6.4	0.0		6775.2	
ROLL	-9.3	-574.0	574.0	0.0	-1255.2	0.0	0.0	79.0	994.9	0.0	173.0	0.0	0.0
PITCH	0.7	-54.4	-54.4	2693.5	-1968.6	0.0	0.0	-898.1	230.4	0.0	15.0	0.0	37.4
YAW	20.8	151.9	-151.9	0.0	2637.1	0.0	0.0	-8.1	-7812.1	0.0	-6657.0	11861.0	-0.0
MR F/A MOM	-21.8												
MR LAT MOM	8.8												
TR F/A MOM	-0.9												
TR LAT MOM	-0.3												

VARII 205.35617 -25.67987 3.36524 -14.76314 5.853691553.30922

	THRUST	H-FORCE	Y-FORCE	TORQUE	IND. V.	CONING	JET THRUST	
MAIN ROTOR	9865.	910.	11.	11821.	7.335	2.235	RIGHT/CENTER	0.
TAIL ROTOR	287.	16.	7.	39.	5.713	1.490	LEFT	0.

FORCE AND MOMENT SUMMARY

	TOTAL	R.WING	L.WING	ELE	FUS	R.JET	L.JET	M.R.	T.R.	GUN	FIN	W/OMR	QTR
X-FORCE	-53.6	-50.1	-50.1	12.6	-171.5	0.0	0.0	-910.4	-16.0	0.0	-23.4	1155.4	
Y-FORCE	5106.3				706.6	0.0	0.0	11.1	286.6	0.0	268.9	3895.0	
Z-FORCE	-3087.3	-192.5	-192.5	153.3	227.9	0.0	0.0	-9865.4	6.5	0.0		6775.2	
ROLL	-40.4	-625.5	625.5	0.0	-1293.7	0.0	0.0	71.1	1002.2	0.0	180.0	0.0	0.0
PITCH	11.0	-58.4	-58.4	2658.7	-2059.3	0.0	0.0	-761.4	235.4	0.0	15.7	0.0	38.6
YAW	-282.1	162.9	-162.9	0.0	2699.8	0.0	0.0	-7.4	-7870.5	0.0	-6925.4	11821.5	-0.0
MR F/A MOM	14.6												
MR LAT MOM	10.8												
TR F/A MOM	-1.5												
TR LAT MOM	8.2												

DELTA

FORCE AND MOMENT SUMMARY

	TOTAL	R.WING	L.WING	ELE	FUS	R.JET	L.JET	M.R.	T.R.	GUN	FIN	W/OMR	QTR
X-FORCE	-53.5	-3.4	-3.4	-0.7	-12.2	0.0	0.0	-32.4	-0.5	0.0	-1.0	-0.0	
Y-FORCE	32.4				21.0	0.0	0.0	-1.1	2.1	0.0	10.4	-0.0	
Z-FORCE	-131.9	-15.9	-15.9	-2.0	6.7	0.0	0.0	-105.0	0.1	0.0		0.0	
ROLL	-31.1	-51.6	51.6	0.0	-38.4	0.0	0.0	-6.9	7.3	0.0	7.0	0.0	0.0
PITCH	10.3	-4.0	-4.0	-36.8	-90.7	0.0	0.0	136.8	5.0	0.0	0.7	0.0	1.2
YAW	-302.9	11.0	-11.0	0.0	62.7	0.0	0.0	0.7	-58.3	0.0	-268.4	-39.6	-0.0
MR F/A MOM	14.6												
MR LAT MOM	10.8												
TR F/A MOM	-1.5												
TR LAT MOM	8.2												

TABLE II

SUMMARY OF STABILITY DERIVATIVES

STABILITY PARTIAL DERIVATIVE MATRICES

	U	W	Q	V	P	R
X-FORCE	-10.04434	-22.76096	581.5625	-4.536231	-378.1006	-10.74737
Z-FORCE	-26.37503	-218.8313	-716.3281	0.3703125	-528.2031	5.000000
PITCH MOMENT	2.054720	-121.3912	-7056.926	-15.25978	2465.263	149.2102
Y-FORCE	0.445938	2.114062	-325.0000	-54.40312	-722.8906	484.2969
ROLL MOMENT	-0.219542	14.01077	-2044.725	9.054884	-4408.254	1054.729
YAW MOMENT	-00.58149	-50.51640	8089.375	179.3735	2028.984	-12868.12
			MAIN ROTOR			
THRUST	20.99297	189.0282	561.2500	-0.5539063	568.2031	1.718750
H-FORCE	0.472901	16.77113	-602.5391	-0.1933594E-01	387.1924	1.088867
F/A FLAPPING	0.4729624E-03	0.7666827E-03	-0.1160814	0.6499291E-04	0.3003836E-01	0.0
Y-FORCE	-0.2172913	2.273594	-316.9780	-4.615293	-646.6658	1.146240
TORQUE	-7.910157	-53.33125	7663.281	0.1914063	-498.0469	-5.546875
LAT FLAPPING	0.8026512E-05	0.3021955E-03	-0.2640314E-01	-0.4203601E-03	-0.1065867	0.0
			TAIL ROTOR			
THRUST	0.4219239	-0.1568848	-5.454102	-6.595976	-75.11230	255.4053
H-FORCE	0.9015465E-01	0.2001972E-01	0.3423119	-0.3239540	-7.624931	1.243534
F/A FLAPPING	0.0	0.0	0.0	-0.4550151E-03	-0.3267164E-01	-0.2743103E-01
Y-FORCE	0.2494564E-01	-0.3451424E-01	-0.7338524	-0.2553881	9.818764	4.276485
TORQUE	0.2419251	-0.4504090E-01	-1.945496	1.528079	3.564453	-10.27252
LAT FLAPPING	0.0	0.0	0.0	-0.3943990E-03	0.3443584E-01	-0.1099745E-01

TABLE III

STABILITY CHARACTERISTICS DATA

LONGITUDINAL MODE

DIMENSIONAL COEFFICIENTS OF CHARACTERISTIC EQUATIONS

U-S**2	U-S	U	ALPHA-S**2	ALPHA-S	ALPHA	THETA-S**2	THETA-S	THETA	F/A CYCLIC	COLLEC.
0.0	245.57	10.694	0.0	0.0	22.781	0.0	-2.8714	33.452	2.5674	-2.4960
0.0	0.0	26.375	0.0	245.63	718.03	0.0	-242.03	-5.7040	7.0591	-20.054
0.0	0.0	-2.0547	0.0	1.0564	121.39	55.565	34.843	0.0	-15.550	6.7998

NON-DIMENSIONAL COEFFICIENTS OF CHARACTERISTIC EQUATIONS

U-S**2	U-S	U	ALPHA-S**2	ALPHA-S	ALPHA	THETA-S**2	THETA-S	THETA	F/A CYCLIC	COLLEC.
0.0	5972.4	1.5974	0.0	0.0	3.4029	0.0	-65.157	4.9968	0.38350	-0.37284
0.0	0.0	3.9347	0.0	5973.8	42.687	0.0	-5492.2	-0.85211	1.0544	-2.9954
0.0	0.0	-0.11538	0.0	9.0072	8.8003	71609.	296.52	0.0	-0.87111	0.35097

CONTROLS FIXED

ROOTS REAL	ROOTS IMAG.	PERIOD	FREQUENCY	T-HALF-SEC	FWD.VEL/THETA MAGN.	FWD.VEL/THETA PHASE	ALPHA/THETA MAGN.	ALPHA/THETA PHASE	LEAD COEF.
-0.27345E-01	0.11791	53.502	0.18070E-01	25.344	1.1022	90.662	0.15989E-01	-44.323	0.33505E 07
-0.76791	1.4454	4.3469	0.23005	0.90856	0.14485	72.832	1.0948	32.541	0.33505E 07

FREQUENCY RESPONSE

DEPENT.VAR.	INDEP. VAR.	REAL1	IMAG1	REAL2	IMAG2	REAL3	IMAG3	GAIN
FWD. VEL.	F/A CYCLIC	-0.517350	0.0	-0.225443	2.83234	-0.225443	-2.83234	2.11747
FWD. VEL.	COLLECTIVE	-0.8163e7	0.0	0.835764E-01	2.19239	0.835764E-01	-2.19239	-2.05861
ANG. OF ATK.	F/A CYCLIC	-0.353030E-01	-0.122632	-0.350308E-01	0.122632	9.03714	0.0	0.787384E-01
ANG. OF ATK.	COLLECTIVE	-0.510122E-01	-0.131280	-0.510122E-01	0.131280	0.922081	0.0	-0.816405E-01
PITCH ANGLE	F/A CYCLIC	-0.255e54E-01	0.0	-1.12956	0.0	0.0	0.0	-0.780507
PITCH ANGLE	COLLECTIVE	-0.330e07E-01	0.0	-7.32854	0.0	0.0	0.0	0.123975

DEP. VAR.	INDEP. VAR.	TAU	DAMP	TAU	DAMP	TAU	DAMP	STATIC GAIN
FWD. VEL.	F/A CYCLIC	0.0	1.93253	0.123870	0.556514E-01	0.0	0.0	278.183
FWD. VEL.	COLLECTIVE	0.0	1.22644	0.207747	-0.347755E-01	0.0	0.0	-20n.724
ANG. OF ATK.	F/A CYCLIC	61.4464	4.30414	0.0	0.0	0.0	-0.110654	-0.108984
ANG. OF ATK.	COLLECTIVE	55.4118	5.14324	0.0	0.0	0.0	-1.38493	0.385292E-01
PITCH ANGLE	F/A CYCLIC	0.0	39.0787	0.0	0.885303	0.0	0.0	-0.709199
PITCH ANGLE	COLLECTIVE	0.0	32.5831	0.0	0.429453	0.0	0.0	0.228599

DENOMINATOR 66.9241 3.76946 0.374350 0.571189 0.0 0.0 0.387571E-01

ALL ROOTS, FREQUENCIES, PERIODS, AND TIME TO HALF OR DOUBLE AMPLITUDE ARE IN REAL SECONDS
ALL MAGNITUDES AND PHASE ANGLES HAVE BEEN DETERMINED FROM ROOTS IN AIR SECONDS
GAINS ARE DETERMINED FROM ROOTS IN REAL SECONDS
ALL STATIC GAINS ARE IN NATURAL UNITS PER INCH OF STICK
T0 = 0.658276-02

TABLE III - Continued

LATERAL MODE

DIMENSIONAL COEFFICIENTS OF CHARACTERISTIC EQUATIONS

BETA-S**2	BETA-S	BETA	PHI-S**2	PHI-S	PHI	R-S**2	R-S	R	LAT CYCLIC	PEDAL
0.0	245.57	54.403	0.0	3.5692	-33.452	0.0	0.0	243.18	1.2719	1.3839
0.0	0.0	-9.0549	17.642	21.765	0.0	0.0	4.3005	-5.2076	8.1468	5.0893
0.0	0.0	-179.37	4.3005	-10.018	0.0	0.0	49.046	63.535	-0.73925	-38.263

NON-DIMENSIONAL COEFFICIENTS OF CHARACTERISTIC EQUATIONS

BETA-S**2	BETA-S	BETA	PHI-S**2	PHI-S	PHI	R-S**2	R-S	R	LAT CYCLIC	PEDAL
0.0	1425.2	8.1263	0.0	20.714	-4.9968	0.0	0.0	1411.3	0.18499	0.20671
0.0	0.0	-0.12973	381.55	12.116	0.0	0.0	93.038	-2.8988	0.11672	0.72915E-01
0.0	0.0	-2.5849	93.008	-5.5765	0.0	0.0	1060.7	65.367	-0.10591E-01	-0.54820

CONTROLS FIXED

ROOTS REAL	ROOTS IMAG.	PERIOD	FREQUENCY	T-HALF-DBL	SIDE SLIP/ROLL ANG. MAGN.	PHASE	YAW ANG./ROLL ANG. MAGN.	PHASE	LEAD COEF.
0.45240E-01	0.0	0.0	0.0	15.321	0.43618E-01	0.0	2.7674	0.0	0.20794E 06
-0.72038	1.7963	3.4978	0.28590	0.91399	3.3133	-82.196	3.1537	92.364	0.20794E 06
-1.4117	0.0	0.0	0.0	0.49099	0.11711	0.0	0.21183	180.01	0.20794E 06

FREQUENCY RESPONSE

DEPENT.VAR.	INDEP. VAR.	REAL1	IMAG1	REAL2	IMAG2	REAL3	IMAG3	GAIN
SDE.SLP.ANG.	LAT CYCLIC	0.148063	-1.12110	0.148063	1.12110	-17.4782	0.0	0.517952E-02
SDE.SLP.ANG.	PEDAL	-0.205645E-01	0.0	-1.18951	0.0	-144.815	0.0	0.963536E-02
ROLL ANGLE	LAT CYCLIC	-0.746479	-1.83147	-0.746479	1.83147	0.0	0.0	0.475630
ROLL ANGLE	PEDAL	-0.258353	-1.74106	-0.258353	1.74106	0.0	0.0	0.489105
YAW RATE	LAT CYCLIC	-0.437152	-1.25582	-0.437152	1.25582	2.35240	0.0	-0.567768E-01
YAW RATE	PEDAL	-0.819342	-0.310663	-0.819342	0.310663	0.320569	0.0	-0.823026

DEP. VAR.	INDEP. VAR.	TAU	DAMP	TAU	DAMP	TAU	DAMP	STATIC GAIN
SDE.SLP.ANG.	LAT CYCLIC	0.761947	-0.231569	0.0	0.0	0.0	0.801397E-01	-0.340370
SDE.SLP.ANG.	PEDAL	0.0	48.6274	0.0	0.840683	0.0	0.690537E-02	-0.822114E-01
ROLL ANGLE	LAT CYCLIC	0.299656	0.381683	0.0	0.0	0.0	0.0	-7.66170
ROLL ANGLE	PEDAL	0.322784	0.166784	0.0	0.0	0.0	0.0	-6.24025
YAW RATE	LAT CYCLIC	0.565548	0.494461	0.0	0.0	0.0	-0.425098	-0.972575
YAW RATE	PEDAL	1.30237	2.13417	0.0	0.0	0.0	-3.11926	-0.834335

DENOMINATOR 0.0 -22.1041 0.263022 0.398939 0.0 0.706347 -0.242822

ALL ROOTS, FREQUENCIES, PERIODS, AND TIME TO HALF OR DOUBLE AMPLITUDE ARE IN REAL SECONDS
ALL MAGNITUDES AND PHASE ANGLES HAVE BEEN DETERMINED FROM ROOTS IN AIR SECONDS
GAINS ARE DETERMINED FROM ROOTS IN REAL SECONDS
ALL STATIC GAINS ARE IN NATURAL UNITS PER INCH OF STICK
T0 = 0.25736E-01

1.201 MINUTES USED IN STAB 1.925 MINUTES TOTAL RUN TIME

TABLE IV

MANEUVER SUBROUTINE OUTPUT DATA

0.510 SECONDS MANEUVER TIME 1.242 MINUTES ELAPSED COMPUTING TIME LB,FT,DEG,SEC UNITS

MAIN ROTOR SHAFT REFERENCE

	O/A1	P/B1				PSI	BETA	FORCES	
VELOCITY	49.372	-178.070	U	200.286	ACCEL	0.0	718.447	THRUST	8874.625
LOCATION	-2.443	-0.693	V	-16.065	VELOCITY	1944.358	-83.616	H-FORCE	894.944
			W	-25.729	LOCATION	271.620	2.127	Y-FORCE	-287.698

FROM	COLLEC	F/A CYC	LAT CYC								
CONTROLS	14.972	0.131	-0.525	CONING	2.625	M.TILT	0.0	TORQ	14317.78	FLAP. LIM.	HUB SPRINGS
OTHER	0.0	0.0	0.0	IND. V	6.311	RPM	324.060	HP	914.27	UPPER 29.500	F/A 0.0
TOTAL	14.972	0.131	-0.525							LOWER -24.000	LAT 0.0

TAIL ROTOR SHAFT REFERENCE

	O/A1	P/B1				PSI	BETA	FORCES	
VELOCITY	-79.243	-37.965	U	200.546	ACCEL	0.0	8874.492	THRUST	276.435
LOCATION	0.123	-0.350	V	-24.617	VELOCITY	9939.586	8.913	H-FORCE	6.612
			W	16.176	LOCATION	29.186	1.222	Y-FORCE	11.565

FROM	COLLEC	F/A CYC	LAT CYC								
CONTROLS	1.931	0.0	0.0	CONING	1.493	M.TILT	0.0	TORQ	37.90	FLAP. LIM.	HUB SPRINGS
OTHER	0.0	0.0	0.0	IND. V	6.572	RPM	1656.597	HP	11.95	UPPER 27.000	F/A 0.0
TOTAL	1.933	0.0	0.0							LOWER -24.000	LAT 0.0

GROUND REFERENCE

	X	Y	Z			SPEED (KTS)	FLT PATH ANGLES	
VELOCITY	202.371	10.853	0.773	DISTANCE	103.3	AIR 120.08	HEADING	3.079
LOCATION	103.251	2.791	-4999.668	ALTITUDE	4999.7	GND 120.08	CLIMB	-0.219

FUSELAGE REFERENCE

	U	V	W	P	Q	R	BODY	EULER ANGLES FROM GROUND	PSI	THETA	PHI
ACCEL	-1.114	-3.643	-4.351	-36.437	2.314	22.144	0.0				
VELOCITY	200.489	-14.620	-25.750	-12.151	1.920	7.807	0.0	VELOCITY	7.587	-1.960	-13.331
								LOCATION	3.515	-8.608	26.536

CONTROLS (PCT)

			L. WING	R. WING	ELE	FIN/RUD	FUSELAGE		C.G. LOC (IN)		G/ST (CG)	G-S	
COLSTK	27.11												
F/A CYCSTK	49.31	ATK	5.796	5.796	-4.075	8.130	ATKY 4.171	STA. LINE	192.00	FWD	0.0	FWD	-0.15
LAT CYCSTK	51.72	CL	0.275	0.275	-0.199	0.294	ATKP -7.319	B. LINE	0.0	LAT	0.0	LAT	-0.12
PEDAL	31.11	CD	0.031	0.031	0.020	0.044		W. LINE	75.97	VERT	0.0	VERT	1.12

JET THRUST		ENGINE			
RIGHT/CENTER	0.0	TORQUE	15011.5	TOTAL HP REQ	926.2
LEFT	0.0	SHAFT HP	926.2	ROTOR BRAKE TORQUE	0.0

FORCE AND MOMENT SUMMARY

	TOTAL	R.WING	L.WING	ELE	FUS	R.JET	L.JET	M.R.	T.R.	GUN	FIN	W/OMR	QTR
X-FORCE	14.9	-47.5	-47.5	11.8	-160.2	0.0	0.0	-894.9	-6.6	0.0	-22.6	1182.5	
Y-FORCE	4423.9				681.0	0.0	0.0	-287.7	276.4	0.0	264.5	3489.7	
Z-FORCE	-1871.0	-181.2	-181.2	144.5	221.9	0.0	0.0	-8874.6	11.6	0.0		6988.1	
ROLL	-1947.3	-589.0	589.0	0.0	-1246.7	0.0	0.0	-1837.7	960.1	0.0	177.0	0.0	0.0
PITCH	615.2	-55.2	-55.2	2506.4	-1973.9	0.0	0.0	-199.9	340.1	0.0	15.1	0.0	37.9
YAW	3229.7	154.2	-154.2	0.0	2612.0	0.0	0.0	191.8	-7543.2	0.0	-6811.6	14817.8	-0.0
MR F/A MOM	-1187.9												
MR LAT MOM	41996.9												
TR F/A MOM	-117.9												
TR LAT MOM	-65.9												

MAIN ROTOR

	BLADE 1	BLADE 2	BLADE 3	BLADE 4	BLADE 5	BLADE 6	BLADE 7
AZIMUTH LOCATION	271.620	91.620	0.0	0.0	0.0	0.0	0.0
FLAPPING ACCEL WRT MAST	718.447	-718.447	0.0	0.0	0.0	0.0	0.0
FLAPPING VELOCITY WRT MAST	-83.616	83.616	0.0	0.0	0.0	0.0	0.0
FLAPPING LOCATION WRT MAST	2.127	3.373	0.0	0.0	0.0	0.0	0.0

TAIL ROTOR

	BLADE 1	BLADE 2	BLADE 3	BLADE 4	BLADE 5	BLADE 6	BLADE 7
AZIMUTH LOCATION	29.186	209.186	0.0	0.0	0.0	0.0	0.0
FLAPPING ACCEL WRT MAST	8874.492	-8874.492	0.0	0.0	0.0	0.0	0.0
FLAPPING VELOCITY WRT MAST	8.913	-8.912	0.0	0.0	0.0	0.0	0.0
FLAPPING LOCATION WRT MAST	1.222	1.778	0.0	0.0	0.0	0.0	0.0

TABLE V

AIRLOADS SUBROUTINE OUTPUT DATA

AZIMUTH	U-SHAFT	V-SHAFT	W-SHAFT	XK	SIN(BETA)	COS(BETA)	BETA DOT
271.62012	200.28595	-16.06529	-25.72855	0.95630	0.03493	0.99939	-36.78943

RAD.STA.	PHI	ALPHA	CL	CD	MACH	LOCAL VI	LOC. LAMBDA	UT	UP
1.00000	0.29517	5.41272	0.50055	0.01521	0.48834	6.31101	-34.36337	545.46338	2.81008
0.95000	0.15813	5.77568	0.52592	0.01568	0.45493	6.31101	-33.93126	508.15723	1.40246
0.90000	-0.00063	6.11692	0.54931	0.01617	0.42153	6.31101	-33.49915	470.85107	-0.00515
0.85000	-0.18671	6.43086	0.57035	0.01667	0.38813	6.31101	-33.06703	433.54468	-1.41277
0.80000	-0.40782	6.70972	0.58851	0.01714	0.35474	6.31101	-32.63493	396.23853	-2.82043
0.75000	-0.67488	6.94266	0.60296	0.01755	0.32136	6.31101	-32.20282	358.93237	-4.22803
0.70000	-1.00386	7.11369	0.61245	0.01785	0.28798	6.31101	-31.77072	321.62622	-5.63567
0.65000	-1.41907	7.19848	0.61505	0.01796	0.25462	6.31101	-31.33861	284.31982	-7.04331
0.60000	-1.95946	7.15809	0.60760	0.01779	0.22127	6.31101	-30.90649	247.01373	-8.45092
0.55000	-2.69154	6.92601	0.58464	0.01717	0.18795	6.31101	-30.47438	209.70758	-9.85854
0.50000	-3.73888	6.37867	0.53597	0.01590	0.15467	6.31101	-30.04228	172.40118	-11.26618
0.45000	-5.35946	5.25809	0.44019	0.01368	0.12148	6.31101	-29.61017	135.09503	-12.67380
0.40000	-8.19415	2.92340	0.24407	0.01046	0.08845	6.31101	-29.17805	97.78888	-14.08142
0.35000	-14.36418	-2.74664	-0.22889	0.01027	0.05589	6.31101	-28.74594	60.48273	-15.48903
0.30000	-36.09361	-23.97606	-0.85969	0.30107	0.02568	6.31101	-28.31384	23.17651	-16.89665
0.25000	-127.66579	-115.04823	0.87075	1.72244	0.02070	6.31101	-27.88173	-14.12970	-18.30429
0.20000	-159.03154	-145.91397	1.03206	0.65751	0.04931	6.31101	-27.44962	-51.43593	-19.71190
0.15000	-166.61333	-152.99573	0.92028	0.43090	0.08167	6.31101	-27.01752	-88.74214	-21.11954
0.10000	-169.86711	-155.74956	0.86547	0.35237	0.11463	6.31101	-26.58540	-126.04837	-22.52718
0.05000	-171.66428	0.0	0.0	0.0	0.14781	6.31101	-26.15329	-163.35458	-23.93478

AZIMUTH	U-SHAFT	V-SHAFT	W-SHAFT	XK	SIN(BETA)	COS(BETA)	BETA DOT
91.62015	200.28595	-16.06529	-25.72855	0.95630	0.05666	0.99839	36.78944

RAD.STA.	PHI	ALPHA	CL	CD	MACH	LOCAL VI	LOC. LAMBDA	UT	UP
1.00000	-4.30598	0.52009	0.06688	0.04369	0.84934	6.31101	-33.90834	946.03931	-71.23235
0.95000	-4.34096	0.98511	0.12260	0.02432	0.81592	6.31101	-33.49899	908.77026	-68.98418
0.90000	-4.37893	1.44714	0.17116	0.01480	0.78250	6.31101	-33.08963	871.50146	-66.73599
0.85000	-4.42029	1.90578	0.21581	0.01419	0.74908	6.31101	-32.68027	834.23242	-64.48782
0.80000	-4.46551	2.36056	0.25742	0.01382	0.71566	6.31101	-32.27090	796.96338	-62.23965
0.75000	-4.51515	2.81091	0.29656	0.01363	0.68224	6.31101	-31.86156	759.69434	-59.99149
0.70000	-4.56992	3.25615	0.33364	0.01360	0.64882	6.31101	-31.45219	722.42529	-57.74332
0.65000	-4.63064	3.69543	0.36892	0.01370	0.61540	6.31101	-31.04283	685.15625	-55.49513
0.60000	-4.69832	4.12775	0.40261	0.01391	0.58198	6.31101	-30.63348	647.88721	-53.24696
0.55000	-4.77426	4.55181	0.43480	0.01422	0.54856	6.31101	-30.22412	610.61816	-50.99879
0.50000	-4.86004	4.96603	0.46556	0.01462	0.51515	6.31101	-29.81476	573.34912	-48.75061
0.45000	-4.95773	5.36834	0.49487	0.01508	0.48173	6.31101	-29.40541	536.08032	-46.50244
0.40000	-5.06997	5.75609	0.52263	0.01560	0.44832	6.31101	-28.99605	498.81128	-44.25427
0.35000	-5.20030	6.12576	0.54868	0.01616	0.41491	6.31101	-28.58669	461.54224	-42.00610
0.30000	-5.35345	6.47261	0.57273	0.01673	0.38150	6.31101	-28.17734	424.27344	-39.75793
0.25000	-5.53600	6.79006	0.59433	0.01730	0.34809	6.31101	-27.76797	387.00439	-37.50977
0.20000	-5.75731	7.06875	0.61278	0.01783	0.31469	6.31101	-27.35861	349.73535	-35.26158
0.15000	-6.03117	7.29489	0.62704	0.01827	0.28129	6.31101	-26.94926	312.46631	-33.01341
0.10000	-6.37880	7.44726	0.63542	0.01855	0.24791	6.31101	-26.53990	275.19727	-30.76524
0.05000	-6.83461	0.0	0.0	0.0	0.21453	6.31101	-26.13054	237.92839	-28.51706

TABLE VI

VECTOR ANALYSIS SUBROUTINE OUTPUT DATA

BELL HELICOPTER 1AM 360/ PROGRAM ASAJ01
HELICOPTER RIGID BODY DYNAMICS ANALYSIS
COMPILED 10/30/69
COMPUTED 03/09/70

11 10276900 HUEY
OUTPUT FIGURES FOR FINAL REPORT
V= 140 KTS GW= 9500 CG= 200

LEAST SQUARES CURVE FIT STARTING AFTER 3.994 SECONDS MANEUVER TIME

FIT1 = AMPLITUDE*SIN(OMEGA*T + PHASE ANGLE) + CONSTANT WITH OMEGA = 0.500 CPS

VARIABLE	AMPLITUDE	PHASE ANGLE (DEGREES)	CONSTANT	COEF OF CORR
Q VELOCITY, TPP1, DEG/SEC	12.849	158.35	0.47288	0.84458
P VELOCITY, TPP1, DEG/SEC	3.6539	4.1135	-0.19593	0.40547
ROTOR THRUST, LB	4531.8	133.01	-84.087	0.99824
F/A FLAPPING, MAST1/TPP1, DEG	2.8155	179.13	-0.59607	0.99917
LATERAL FLAPPING, PAST1/TPP1, DEG	0.24511	139.62	0.84244E-01	0.92941
Q VELOCITY, BODY AXES, DEG/SEC	17.992	131.07	0.46954	0.99935
BODY PITCH WRT. FLIGHT PATH, DEG	4.1208	70.149	-11.621	0.99971

AMPLITUDE AND PHASE ANGLE COMPARISONS

VARIABLES		AMPLITUDE RATIO	PHASE ANGLE DIFFERENCE
Q VELOCITY, TPP1, DEG/SEC	/ BODY PITCH WRT. FLIGHT PATH, DEG	3.1180	88.206
ROTOR THRUST, LB	/ BODY PITCH WRT. FLIGHT PATH, DEG	1099.7	62.863
F/A FLAPPING, MAST1/TPP1, DEG	/ BODY PITCH WRT. FLIGHT PATH, DEG	0.68323	108.99
LATERAL FLAPPING, MAST1/TPP1, DEG	/ BODY PITCH WRT. FLIGHT PATH, DEG	0.59481E-01	69.473

VARIABLE 'A' AS A LINEAR COMBINATION OF VARIABLES 'B' AND 'C'.

A = KB*B + KC*C + KD

VARIABLE	NAME	COEFFICIENT
A	F/A FLAPPING, MAST1/TPP1, DEG	
B	Q VELOCITY, BODY AXES, DEG/SEC	0.16939
C	BODY PITCH WRT. FLIGHT PATH, DEG	-0.58232
	CONSTANT	-7.4425

TABLE VII

FUSELAGE EQUATIONS

Aerodynamics

$$L_f = q' \left(XFS20 + XFS21\ \alpha_f \right)$$

$$D_f = q' \left(XFS22 + XFS23\ \alpha_f + XFS24\ \alpha_f^2 + XFS25\ \beta_f^2 + XFS32\ \cos^3\beta_m \right)$$

$$Y_f = q' \left(XFS26 + XFS27\ \beta_f + XFS28\ \beta_f^2 \right)$$

$$M_f = q' \left| \left(XFS15 + XFS16\ \alpha_f \right) + XFS32\ \cos^3\beta_m\ (XFS31 - XMR10)/12 \right|$$

$$N_f = q' \left(XFS17 + XFS18\ \beta_f \right)$$

In addition to the above fuselage moments, the fuselage forces will contribute to moments if the fuselage aerodynamic center is different from the center of gravity by acting through the appropriate moment arms. The following equation indicates this effect on roll moment of the fuselage side force, Y_f.

$$L_f = Y_f\ (XFS04 - XFS07)/12$$

Center of Gravity**

$$BL = XFS06$$

$$SL = XFS05 + \frac{XFS29}{XFS01} \left| (XMR10 - XFS31)\ \sin\beta_m + (XMR08 - XFS30)\ \left(1 - \cos\beta_m \right) \right|$$

$$WL = XFS07 + \frac{XFS29}{XFS01} \left| (XMR10 - XFS31) \left(1 - \cos\beta_m \right) - (XMR08 - XFS30)\ \sin\beta_m \right|$$

NOTE: See Volume II for explanation of symbols.

**Assumes rotor masts tilt together and the c.g. buttline does not vary with mast tilt.

TABLE VIII

AIRFOIL CHARACTERISTICS INPUT DATA

	Word	Parameter	Units
Card A	YXX* 1	Critical Mach Number for drag divergence for α=0	Nondim
	2	Mach number (M_s) for lower boundary of supersonic region	Nondim
	3	Maximum C_L, normal flow, M=0	Nondim
	4	Coefficient of Mach number (M) in $C_{L_{MAX}}$ Equation, normal flow	Nondim
	5	Coefficient of M^2 in $C_{L_{MAX}}$ Equation, Normal Flow	Nondim
	6	Coefficient of M^3 in $C_{L_{MAX}}$ Equation, normal flow	Nomdim
	7	Maximum C_L, reverse flow, M=0	Nondim
Card B	8	Coefficient of Mach number (M) in $C_{L_{MAX}}$ Equation, Reverse Flow	Nondim
	9	Coefficient of M^2 in $C_{L_{MAX}}$ Equation Reverse Flow	Nondim
	10	Coefficient of M^3 in $C_{L_{MAX}}$ Equation, Reverse flow	Nondim
	11	Tail boom bending coefficient for correction of C_L of a fin or elevator	Rad/lb of Lift
	12	Drag coefficient for α=0 and M=0	Nondim
	13	Coefficient of α in nondivergent drag equation	/deg
	14	Coefficient of α^2 in nondivergent drag equation	/deg^2
Card C	15	Coefficient used in supersonic drag equation	Nondim

TABLE VIII - Continued

Card C	16	Maximum drag coefficient for M<1; also value of drag coefficient for 1<M<M_s	Nondim
	17	2 dimensional lift curve slope for M=0	/deg
	18	Aspect Ratio	Nondim
	19	Not Used	-
	20	Not Used	-
	21	Not Used	-

* Note: YXX represents the word for the appropriate surface; ie: such as YFN for fin, YWG for wing, YMR for main rotor.

TABLE IX

CONTROL SYSTEM LINKAGES

Control or System	Controlled Elements: Horizontal Stabilizer Incidence	Vertical Stabilizer Incidence	Wing Incidence: Right	Wing Incidence: Left	Level of Auxiliary Thrust	Collective Pitch	Main (forward, right) Rotor: Longitudinal Cyclic Pitch	Main (forward, right) Rotor: Lateral Cyclic Pitch	Main (forward, right) Rotor: Collective Pitch	Tail (aft, left) Rotor: Longitudinal Cyclic Pitch	Tail (aft, left) Rotor: Lateral Cyclic Pitch	Configuration
Collective pitch lever	x		x	x	x	x						single
	x		x	x	x	x			x			tandem
	x		x	x	x	x			x			composite
F/A cyclic stick	x						x					single
	x					x	x		x	x		tandem
	x						x	x		x	x	composite
Lateral cyclic stick			+x	-x				x				single
			+x	-x				x			x	tandem
			+x	-x		x	x	x	x	x	x	composite
Pedal		x							x			single
		x						x			x	tandem
		x				x	x		x	x		composite
Bobweight						x						single
						x			x			tandem, comp.
Rotor speed governor						x						single
						x			x			tandem, comp.
Mast tilt						x	x	x	x	x	x	composite

TABLE X

EQUATIONS OF MOTION

1. Flight Path

$$X = m(\dot{U} + qW - rV)$$

$$Y = m(\dot{V} + rU - pW)$$

$$Z = m(\dot{W} + pV - qU)$$

$$L = I_x\dot{p} - I_{xz}\dot{r} + qr(I_z - I_y) - I_{xz}pq$$

$$M = I_y\dot{q} + rp(I_x - I_z) + I_{xz}(p^2 - r^2)$$

$$N = I_z\dot{r} - I_{xz}\dot{p} + pq(I_y - I_x) + I_{xz}qr$$

$$\dot{\theta} = q\cos\phi - r\sin\phi$$

$$\dot{\phi} = p + q\sin\phi\tan\theta + r\cos\phi\tan\theta$$

$$\dot{\psi} = (q\sin\phi + r\cos\phi)/\cos\theta$$

$$\begin{Bmatrix}\dot{x}\\ \dot{y}\\ \dot{z}\end{Bmatrix} = \begin{bmatrix}\cos\psi\cos\theta & \cos\psi\sin\theta\sin\phi - \sin\psi\cos\phi & \cos\psi\sin\theta\cos\phi + \sin\psi\sin\phi\\ \sin\psi\cos\theta & \sin\psi\sin\theta\sin\phi + \cos\psi\cos\phi & \sin\psi\sin\theta\cos\phi - \cos\psi\sin\phi\\ -\sin\theta & \cos\theta\sin\phi & \cos\theta\cos\phi\end{bmatrix}\begin{Bmatrix}U\\ V\\ W\end{Bmatrix}$$

2. Rotors

$$\text{Torque Supplied} = I_{\text{torsional}}\dot{\Omega} + \text{Torque Required}$$

REFERENCES

1. Blankenship, B. L. and K. W. Harvey, A Digital Analysis for Helicopter Performance and Rotor Blade Bending Moments, Journal of the American Helicopter Society, October, 1962, Vol. 7, No. 4.

2. Duhon, M. J., K. W. Harvey and B. L. Blankenship, Computer Flight Testing of Rotorcraft, Journal of the American Helicopter Society, October, 1965.

3. Contract No. DA44-177-AMC-308(T), Analytical Study of Helicopter Gust Response at High Forward Speeds, June, 1965.

4. Blankenship, B. L. and B. Bird, Program C81-11 Rotorcraft Flight Simulation, BHC Report 599-068-900, January, 1967.

5. Bird, B. J. and B. L. Blankenship, Program AGAJ68, Rotorcraft Flight Simulation, BHC Report 599-068-904, September, 1969.

6. Contract No. DAAJ02-67-C-0044, Exploratory Definition Phase, Composite Aircraft, March, 1967.

7. Gessow, A., Equations and Procedures for Numerically Calculating the Aerodynamic Characteristics of Lifting Rotors, NACA Technical Note 3747, October 1956.

8. Blankenship, B. L., Bell Helicopter IBM 7070 Program A63: Rotor Aerodynamic Performance and Distributed Airloads, Bell Helicopter Company Report No. 8010-099-003, June 28, 1962.

9. Livingston, C. L., Rotor Induced Velocity, BHC IOM 81:CLL:am-838, October 7, 1966.

10. Drees, J. M., A Theory of Airflow Through Rotors and Its Application to Some Helicopter Problems, The Journal of the Helicopter Society of Great Britain, Vol. 3, No. 2, 1949.

11. Duhon, J. M., Wing Lift "Carry-over" as a Function of the Wing Span to Fuselage Width Ratio, BHC IOM 81:JMD:sf-211, October 29, 1965.

12. Etkin, B., Dynamics of Flight, John Wiley & Sons, Inc. New York, 1959.

13. Ellison, D. E., and Hoak, D. E., USAF Stability and Control Datcom, Flight Control Division, AFFDL, Wright-Patterson AFB, Ohio, October 1960, Revised August 1968.

REFERENCES

14. Nielsen, K. L., Methods in Numerical Analysis, The MacMillan Co., 1957 (pp 232-242).

15. Gessow, A. and G. C. Meyer, Jr., Aerodynamics of the Helicopter, the MacMillan Co., 1952.

16. Seckel, E., Stability and Control of Airplanes and Helicopters, Academic Press, N.Y., 1964.

UNCLASSIFIED

Security Classification

DOCUMENT CONTROL DATA - R & D

(Security classification of title, body of abstract and indexing annotation must be entered when the overall report is classified)

1. ORIGINATING ACTIVITY *(Corporate author)*

Bell Helicopter Company
Fort Worth, Texas 76101

2a. REPORT SECURITY CLASSIFICATION
Unclassified

2b. GROUP

3. REPORT TITLE

A STABILITY AND CONTROL PREDICTION METHOD FOR HELICOPTERS AND STOPPABLE ROTOR AIRCRAFT -- VOLUME I

4. DESCRIPTIVE NOTES *(Type of report and inclusive dates)*
Final Report

5. AUTHOR(S) *(First name, middle initial, last name)*

Charles L. Livingston

6. REPORT DATE	7a. TOTAL NO. OF PAGES	7b. NO. OF REFS
February 1970	74	16

8a. CONTRACT OR GRANT NO.
F33615-69-C-1121

b. PROJECT NO. 8219

c. Task No. 821907

d.

9a. ORIGINATOR'S REPORT NUMBER(S)

9b. OTHER REPORT NO(S) *(Any other numbers that may be assigned this report)*
AFFDL-TR-69-123, Volume 1

10. DISTRIBUTION STATEMENT

This document has been approved for public release and sale; its distribution is unlimited.

11. SUPPLEMENTARY NOTES

12. SPONSORING MILITARY ACTIVITY

Air Force Flight Dynamics Laboratory
Wright-Patterson AFB, Ohio 45433

13. ABSTRACT

This report describes a mathematical model of rotorcraft that may be used to determine characteristics of performance, stability, response, and rotor blade loads. The complexity of the equations used requires the use of a digital computer for efficient solution. This four volume report describes the computer program in detail and illustrates the method of computing rotorcraft characteristics by specific example.

This volume presents an overview of the computer program capabilities and describes the formulation of the mathematical model. The second and third volumes present sample cases, detailed input and output formats, and cross-reference indices of FORTRAN variable and subroutine names and usage. A complete FORTRAN listing comprises all of the fourth volume.

DD FORM 1 NOV 65 1473

UNCLASSIFIED

Security Classification

14. KEY WORDS	LINK A		LINK B		LINK C	
	ROLE	WT	ROLE	WT	ROLE	WT
Helicopter Stability and Control Stoppable Rotor Aircraft Stability and Control V/STOL Aircraft Rotorcraft Simulation						